British Journal of Pharmacology

DOI:10.1111/j.1476-5381.2010.01096.x
www.brjpharmacol.org

RESEARCH PAPER

Characterization of RO4583298 as a novel potent, dual antagonist with *in vivo* activity at tachykinin NK_1 and NK_3 receptors

P Malherbe[1], F Knoflach[1], MC Hernandez[1], T Hoffmann[2], P Schnider[2], RH Porter[3], JG Wettstein[1], TM Ballard[1], W Spooren[3] and L Steward[1]

[1]*Discovery Research CNS, F. Hoffmann-La Roche Ltd., Basel, Switzerland,* [2]*Discovery Research Medicinal Chemistry, F. Hoffmann-La Roche Ltd., Basel, Switzerland, and* [3]*Translational Medicine, F. Hoffmann-La Roche Ltd., Basel, Switzerland*

Correspondence
Dr P Malherbe, F. Hoffmann-La Roche Ltd., Functional Neuroscience, Bldg. 69/333, CH-4070 Basel, Switzerland.
E-mail: parichehr.malherbe@roche.com

Keywords
RO4583298; neurokinin; dual NK_1/NK_3 antagonist; senktide; inositol phosphate accumulation; Schild analysis; firing frequency; dopaminergic neurone; GR73632; gerbil foot tapping, mouse tail whips

Received
21 May 2010
Revised
10 September 2010
Accepted
10 October 2010

BACKGROUND AND PURPOSE

Clinical results of osanetant and talnetant (selective-NK_3 antagonists) indicate that blocking the NK_3 receptor could be beneficial for the treatment of schizophrenia. The objective of this study was to characterize the *in vitro* and *in vivo* properties of a novel dual NK_1/NK_3 antagonist, RO4583298 (2-phenyl-N-(pyridin-3-yl)-N-methylisobutyramide derivative).

EXPERIMENTAL APPROACH

RO4583298 *in vitro* pharmacology was investigated using radioligand binding ([^{3}H]-SP, [^{3}H]-osanetant, [^{3}H]-senktide), [^{3}H]-inositol-phosphate accumulation Schild analysis (SP- or [MePhe^7]-NKB-induced) and electrophysiological studies in guinea-pig substantia nigra pars compacta (SNpc). The *in vivo* activity of RO4583298 was assessed using reversal of GR73632-induced foot tapping in gerbils (GFT; NK_1) and senktide-induced tail whips in mice (MTW; NK_3).

KEY RESULTS

RO4583298 has a high-affinity for NK_1 (human and gerbil) and NK_3 (human, cynomolgus monkey, gerbil and guinea-pig) receptors and behaves as a pseudo-irreversible antagonist. Unusually it binds with high-affinity to mouse and rat NK_3, yet with a partial non-competitive mode of antagonism. In guinea-pig SNpc, RO4583298 inhibited the senktide-induced potentiation of spontaneous activity of dopaminergic neurones with an apparent non-competitive mechanism of action. RO4583298 (p.o.) robustly blocked the GFT response, and inhibited the MTW.

CONCLUSIONS AND IMPLICATIONS

RO4583298 is a high-affinity, non-competitive, long-acting *in vivo* NK_1/NK_3 antagonist; hence providing a useful *in vitro* and *in vivo* pharmacological tool to investigate the roles of NK_1 and NK_3 receptors in psychiatric disorders.

Abbreviations

$5\text{-}HT_{2A}$, 5-hydroxytryptamine (serotonin) type 2A receptor; cm, cynomolgus monkey; D_2, dopamine 2 receptor; DA, dopamine; g, gerbil; GFT, gerbil foot tapping; gp, guinea-pig; GPCRs, G-protein coupled receptors; h, human; IP, inositol phosphates; m, mouse; MTW, mouse tail whips; NK, neurokinin receptor; NK_1, neurokinin 1 receptor; NK_2, neurokinin 2 receptor; NK_3, neurokinin 3 receptor; NKA, neurokinin A; NKB, neurokinin B; r, rat; SNpc, substantia nigra pars compacta; SP, substance P; VTA, ventral tegmental area

Introduction

The neurokinin (also called tachykinin) peptide family are composed of substance P (SP, RPKPQQFFGLM-NH2), neurokinin A (NKA, HKTDSFVGLM-NH2) and neurokinin B (NKB, DMHDFFVGLM-NH2), which share a common C-terminal sequence, FXGLM-NH_2. These peptides act as neurotransmitters/neuromodulators and elicit their effects through three types of neurokinin receptors, NK_1, NK_2 and NK_3 (nomenclature follows Alexander *et al.*, 2008). The NK receptors belong to the class A family (rhodopsin-like) of G-protein-coupled receptors (GPCRs) that are coupled via $G_{q/11}$ to the activation of phospholipase C-IP3/DAG signalling pathway leading to an elevation of intracellular Ca^{2+} levels. The tachykinins have different rank order of potencies at the NK receptors: SP > NKA > NKB for the NK_1, NKA > NKB > SP for the NK_2 and NKB > NKA > SP for the NK_3 (Almeida *et al.*, 2004).

NK receptors have been implicated in the pathology of psychiatric diseases such as depression, anxiety and schizophrenia, as well as other diseases such as bronchial asthma, gastrointestinal disorders, inflammatory bowel syndrome and overactive bladder (Lecci and Maggi, 2003; Quartara *et al.*, 2009). NK receptors are distributed throughout the CNS and in peripheral tissue including gut, lung, bladder and bone marrow. Comparative studies using [^{3}H]-senktide autoradiography revealed differences in the CNS localization of NK_3 among rat, gerbil and guinea pig (Langlois *et al.*, 2001), and between some of these species and primates (Nagano *et al.*, 2006). However, the expression of NK_3 (by *in situ* hybridization and NKB/senktide autoradiography) is generally detected in brain regions that include cortex, various nuclei of the amygdala, the hippocampus and midbrain structures (Stoessl, 1994; Shughrue *et al.*, 1996; Langlois *et al.*, 2001; Rigby *et al.*, 2005). NK_3 receptor expression in the human brain has been demonstrated in the prefrontal and visual cortex by immunohistochemistry (Mileusnic *et al.*, 1999a,b; Tooney *et al.*, 2000). NK_3 immunoreactivity has also been shown in human hypothalamus (Koutcherov *et al.*, 2000). At the cellular level, NK_3 receptors are found on the cell surface of major dopamine cell groups within midbrain regions such as substantia nigra (A9), ventral tegmental area and nucleus raphe linealis (A10) (Stoessl, 1994; Langlois *et al.*, 2001). Notably, these are the regions that are involved in psychosis and are proposed to be the site for therapeutic effects of antipsychotic drugs (Harrison, 1999).

Among NK receptors, NK_3 receptors are of particular interest due to their possible role in the pathophysiology of schizophrenia (Spooren *et al.*, 2005; Meltzer and Prus, 2006). Preclinical studies have demonstrated the involvement of NK_3-mediated activation in the release of dopamine, especially in ventral and dorsal striatal regions (Marco *et al.*, 1998). Osanetant (SR 142801) and talnetant (SB 223412), two potent non-peptide antagonists of the NK_3 receptor (Emonds-Alt *et al.*, 1995; Sarau *et al.*, 1997), have been investigated in schizophrenia patients in randomized double-blind placebo controlled phase II clinical trials, and were demonstrated to induce a significant improvement in positive symptoms (Meltzer *et al.*, 2004; Evangelista, 2005; Spooren *et al.*, 2005). Interestingly, acute administration of talnetant has produced significant increases in extracellular dopamine and noradrenaline in the medial prefrontal cortex of guinea pigs (Dawson *et al.*, 2008). Moreover, the genetic disruption of NK_3 expression has been shown to improve performance in several cognition tests, including acquisition of active avoidance, Morris water maze and delayed match to position task (Nordquist *et al.*, 2008a). Recent clinical investigation of talnetant in healthy volunteers has shown that it slightly improved visuomotor coordination and vigilance (Liem-Moolenaar *et al.*, 2010).

Neuroanatomical localization has shown that SP and NK_1 receptors are highly expressed in CNS areas that are known to be involved in the modulation of stress, anxiety and mood disorders, such as the cingulate cortex, caudate putamen, nucleus accumbens, septum, hippocampus, amygdala, various hypothalamic areas, periaqueductal gray, dorsal raphe nucleus and locus coeruleus (Ribeiro-da-Silva and Hokfelt, 2000; Rigby *et al.*, 2005). The NK_1 expressing neurones in the neocortex, hippocampus and amygdala have been demonstrated to be GABA-ergic interneurones (Acsady *et al.*, 1997; Maubach *et al.*, 2001). Furthermore, *in vitro* electrophysiological studies in the rat hippocampus have indicated that SP can facilitate the inhibitory synaptic input to pyramidal neurones (Ogier and Raggenbass, 2003). SP signalling plays a major role in the modulation of stress responses and in the regulation of affective behaviour. It has been shown that various emotional stressors increase SP efflux in discrete forebrain areas such as amygdala and septum (Ebner *et al.*, 2008). The pharmacological blockade or genetic disruption of NK_1 expression has been shown to result in a marked reduction of anxiety and stress-related responses and also increased 5-HT-mediated function (Santarelli *et al.*, 2001; Blier *et al.*, 2004). Anatomical (high level of substance P in dorsal spinal roots), physiological and behavioural studies in animals using NK_1 antagonists, also results from knockout mice, all suggested a central role of substance P and the NK_1 receptor in pain transmission (Otsuka and Yoshioka, 1993; Cao *et al.*, 1998; Quartara *et al.*, 2009). Nevertheless, aprepitant (also known as Emend or MK-869) was shown to be ineffective against acute dental pain and neuropathic pain in clinical trials (Hill, 2000; Urban and Fox, 2000). Although the NK_1 receptor antagonists aprepitant, L-759274 and CP-122,721 were shown to reduce symptoms of depression in phase II studies, this could not be confirmed for aprepitant in a phase III trial (Ebner *et al.*, 2009). Aprepitant has since been approved for clinical use in the treatment of chemotherapy-induced emesis (Quartara *et al.*, 2009). Several NK_1 receptor antagonists are currently in clinical development for depression and other psychiatric disorders, such as anxiety (Ebner *et al.*, 2009).

Based on this evidence, it is hypothesized that the combination of NK_3 and NK_1 receptor antagonism may provide a therapeutic benefit for both the positive and negative symptoms associated with schizophrenia; and an improved side effect profile over existing antipsychotics. The objective of the current study was to provide an *in vitro* and *in vivo* characterization of a novel NK_1/NK_3 antagonist, which originated from an internal drug discovery programme (Peters *et al.*, 2010). The biochemical and electrophysiological characteristics of RO4583298, its mode of antagonism and a comparison with known selective NK_1 and NK_3 antagonists in various species is reported. Our data show that RO4583298 is a potent

dual NK_1/NK_3 antagonist with apparent non-competitive mode of antagonism at both receptors in a recombinant and native preparation (electrophysiological recordings in guinea-pig midbrain slices) and that it blocks in a dose-dependent manner both NK_1- and NK_3-mediated *in vivo* effects (gerbil foot tapping and mouse tail whip behaviours) induced by selective NK_1 and NK_3 agonists.

Methods

Plasmids, cell culture and membrane preparation

cDNAs encoding for gerbil NK_1 (gNK_1, accession no.AJ884917), human NK_1 (hNK_1, accession no. P25103), human NK_2 (hNK_2, accession no: P21452), cynomolgus monkey NK_3 ($cmNK_3$, in-house sequence), gerbil NK_3 (gNK_3, accession no.AM157740), guinea-pig NK_3 ($gpNK_3$, accession no. P30098), human NK_3 (hNK_3, accession no. P29371), mouse NK_3 (mNK_3, accession no. P47937) and rat NK_3 (rNK_3, accession no. p16177) were isolated by RT-PCR from a midbrain cDNA library and were subcloned into pCI-Neo expression vectors (Promega Corporation, Madison, WI).

Human embryonic kidney (HEK) 293 cells were transfected as previously described (Malherbe *et al.*, 2008). After 48 h post-transfection, cells were harvested and washed three times with ice-cold phosphate buffered saline and frozen at –80°C. The pellet was suspended in ice-cold 50 mmol·L^{-1} Tris-HCl pH 7.4 buffer containing 10 mmol·L^{-1} EDTA (10× volume) and homogenized with a polytron (Kinematica AG, Basel, Switzerland) for 30 s at 16 000 r.p.m. After centrifugation at 48 000× *g* for 30 min at 4°C, the pellet was resuspended in ice-cold 10 mmol·L^{-1} Tris pH 7.4 buffer containing 0.1 mmol·L^{-1} EDTA (10× volume), homogenized and recentrifuged as described earlier. The pellet was finally resuspended in ice-cold 10 mmol·L^{-1} Tris pH 7.4 buffer containing 0.1 mmol·L^{-1} EDTA and 10% sucrose (5× volume). The membrane homogenate was frozen at –80°C before use.

Radioligand binding

After thawing, the membrane homogenates were centrifuged at 48 000× *g* for 10 min at 4°C, the pellets were resuspended in the binding buffer. The assay buffers consisted of: for NK_1: 50 mmol·L^{-1} Hepes, 3 mmol·L^{-1} $MnCl_2$, 2 µmol·L^{-1} phosphoramidon, 16.8 µmol·L^{-1} Leupeptin, 0.04% BSA binding buffer at pH 7.4; NK_2: 50 mmol·L^{-1} Tris-HCl, 3 mmol·L^{-1} $MnCl_2$, 4 µg·mL^{-1} Chymostatin, 0.04% BSA at pH 7.4, and NK_3: 50 mmol·L^{-1} Tris-HCl, 4 mmol·L^{-1} $MnCl_2$, 1 µmol·L^{-1} phosphoramidon, 0.1% BSA at pH 7.4. Final assay concentration for hNK_1, gNK_1 and hNK_2 expressing membranes was 2.5 µg protein per well, for h, cm, g and gp NK_3 expressing membranes 5 µg protein per well, and for m and r NK_3 expressing membranes 80 µg protein per well. Saturation isotherms were determined by addition of various concentrations of radioligand [^{3}H]-SP (NK_1; 0.04 to 18 nmol·L^{-1}), [^{3}H]-SR48968 (NK_2; 0.07 to 27 nmol·L^{-1}), [^{3}H]-osanetant (NK_3; 0.009 to 3 nmol·L^{-1}) or [^{3}H]-senktide (0.1 to 50 nmol·L^{-1}) to membranes (in a total reaction volume of 500 µL) for 90 min, respectively, at room temperature (RT). Non-specific binding was determined with 10 µmol·L^{-1} CP-96 345 (NK_1), 10 µmol·L^{-1} MDL 105 212 (NK_2) and 10 µmol·L^{-1} SB 222200 (NK_3), respectively. At the end of the incubation, membranes were filtered onto 96-well white microplates (preincubated 1 h in 0.3% polyethylenimine + 0.1% BSA) with a bonded GF/C filter for [^{3}H]-SP, [^{3}H]-SR48968 and [^{3}H]-osanetant binding or GF/B filter for [^{3}H]-senktide binding (PerkinElmer Life and Analytical Sciences, Waltham, MA), with a FilterMate-96 well harvester (PerkinElmer Life and Analytical Sciences) and washed four times with ice-cold 50 mmol·L^{-1} Tris-HCl, pH 7.4 buffer. The radioactivity on the filter was counted (5 min) on a Packard Top-Count microplate scintillation counter with quenching correction after addition of 45 µL of microscint 40 (Canberra Packard S.A., Zürich, Switzerland) and 1 h agitation. Saturation experiments were analysed by Prism 5.0 (GraphPad software, San Diego, CA) using the rectangular hyperbolic equation derived from the equation of a bimolecular reaction and the law of mass action, $B = (B_{max} * [F])/(K_D + [F])$, where B is the amount of ligand bound at equilibrium, B_{max} (the maximum number of binding sites) is the specific binding extrapolated to very high concentrations of radioligand, [F] is the concentration of free ligand and K_D (the ligand dissociation constant) is the radioligand concentration needed to achieve a half-maximum binding at equilibrium. For inhibition experiments, membranes were incubated with radioligand at a concentration equal to K_D of the radioligand and 10 concentrations of the competing compound (0.0003–10 µmol·L^{-1}). The IC_{50} values (inhibition concentration at which 50% specific binding of the radioligand was displaced) were derived from the inhibition curve using a sigmoidal dose-response (variable slope), which is also known as a four-parameter/nonlinear regression analysis (graphPad prism 5) as shown in the equation $Y = Y_{min} + (Y_{max} - Y_{min})/(1 + 10\text{^}((LogIC_{50} - X)*n_H))$, where Y is the % specific binding, Y_{min} is the minimum Y, Y_{max} is the maximum Y, X is the concentration of the competing compound and n_H is the slope of the curve (the Hill Coefficient). The affinity constant (K_i) values were calculated using the Cheng-Prussoff equation $K_i = IC_{50}/(1 + [L]/K_D)$ where [L] is the concentration of radioligand and K_D is its dissociation constant at the receptor, derived from the saturation isotherm. The K_i is also expressed logarithmically as a pK_i.

[^{3}H]-inositol phosphate (IP) accumulation assay

[^{3}H]-IP accumulation was measured, as described previously, with the following adaptations (Malherbe *et al.*, 2009). HEK293 cells were transfected with various NK cDNAs in pCI-Neo using Lipofectamine Plus™ reagent (Invitrogen) according to the manufacturer's instructions. After 24 h post-transfection, cells were washed twice in labelling medium: Dulbecco's modified Eagle's medium without inositol (MP Biomedicals, Irvine, CA), 10% foetal calf serum, 1% penicillin/streptomycin, and 2 mmol·L^{-1} glutamate. Cells were seeded at 8×10^4 cells per well in poly-D-lysine–treated 96-well plates in the labelling medium supplemented with 5 µCi·mL^{-1} myo-[1,2-^{3}H]-inositol. On the day of assay (48 h post-transfection), cells were washed three times with the buffer (1× HBSS, 20 mmol·L^{-1} HEPES, pH 7.4) and then incubated for 10 min at RT in assay buffer (1× HBSS, 20 mmol·L^{-1} HEPES, pH 7.4, plus 8 mmol·L^{-1} LiCl to prevent phosphotidyl-inositide breakdown) prior to the addition of

agonists or antagonists. Antagonists were incubated for 20 min at 37°C prior to stimulation with the agonist, either SP (NK_1) or [MePhe^7]NKB (NK_3), at concentrations ranging from 1 µmol·L^{-1} to 0.01 nmol·L^{-1}. For competitive or non-competitive antagonism assessment, Schild analyses were performed. The agonist curves were generated in the presence of increasing concentrations of antagonist and the shift in agonist EC_{50} or depression in maximum response was determined. After 45 min incubation at 37°C with the agonist, the assay was terminated by the aspiration of the assay buffer and the addition of 100 µL 20 mmol·L^{-1} formic acid to lyse the cells. After the sample had been shaken for 30 min at 23°C, a 40 µL aliquot was mixed with 80 µL of yttrium silicate RNA binding SPA beads (12.5 mg·mL^{-1}; bind the inositol phosphates but not the inositol) and then shaken for 30 min at 23°C. Assay plates were centrifuged for 2 min at 750× *g* prior to counting on a Packard Top-count microplate scintillation counter with quenching correction (PerkinElmer Life and Analytical Sciences). For PI hydrolysis, activation and inhibition curves were fitted according to the equation: y = A + ((B – A)/((1 + ((C/x)^D)))), where A is y_{min}, B is y_{max}, C is EC_{50} and D is the Hill slope factor, using ExcelFit 3.0 (IDBS software).

Electrophysiology in guinea-pig midbrain slices

Guinea-pigs (6 to 10 days old) were anaesthetized in a 2.5% isoflurane/96.5% oxygen mixture for 2 min and decapitated, according to the approved procedure by the local institutional animal welfare committee. The brain was quickly removed and coronal midbrain slices (250 µmol·L^{-1} thick) containing the substantia nigra pars compacta (SNpc) were cut with a VT1000S vibratome (Leica, Wetslar, Germany) in an ice-cold solution containing (in mmol·L^{-1}) glycerol 250, KCl 2.5, $MgCl_2$ 1.2, $CaCl_2$ 2.4, NaH_2PO_4 1.2, $NaHCO_3$ 26, D-glucose 11 gassed with a mixture of 95% O_2 and 5% CO_2 (335 mosmol L^{-1}). Immediately after being cut, the slices were transferred for 20 min to warm artificial cerebrospinal fluid (ACSF; 35°C) containing (in mmol·L^{-1}) NaCl 119.0, KCl 2.5, $MgCl_2$ 1.3, $CaCl_2$ 2.5, NaH_2PO_4 1, $NaHCO_3$ 26.2, D-glucose 11 gassed with a mixture of 95% O_2 and 5% CO_2 (295 mosmol L^{-1}) and then stored for later use at room temperature. For electrophysiological recordings, a slice was transferred to the recording chamber (volume ~1 mL) containing gassed ACSF held at 35°C and perfused at a rate of 2 mL·min^{-1}. Loose patch recordings were made from dopaminergic (DA) neurones identified visually using a microscope equipped with infrared differential interference contrast optics (Olympus, Basel, Switzerland) and located in the SNpc at the level of the medial terminal nucleus of the accessory optic tract. A neurone was considered DA if it had a regular firing pattern (0.5–2 Hz), a broad (>2 ms), triphasic action potential (Grace and Onn, 1989) and was sensitive to quinpirole (100 nmol·L^{-1}), dopamine receptor agonist. Recoding pipettes were pulled from thin-wall borosilicate glass pipette (Clark GCT150, Warner Instruments, LLC, Hamden, CT) filled with ACSF. Signals were filtered (1 Hz high- and 2 KHz low-pass) and amplified with a Multiclamp 700A amplifier (Molecular Devices, Sunnyvale, CA) digitized at 10 kHz with a DigiData 1200 interface and stored on a personal computer with the pClamp 9.0 data acquisition software (both Molecular Devices). Action potentials were detected by means of threshold search using the Clampfit analysis program (Molecular Devices). The firing frequencies (action potentials·s^{-1}) were calculated in bins of 1 min. Values are given as ±SEM; *n* represents the number of neurones recorded. In concentration-response experiments, increasing concentrations of senktide were perfused for at least 4 min in a consecutive manner. For each senktide concentration, maximum firing frequencies were measured and plotted as a function of the concentration. Firing frequencies from each recorded neurone were fitted with the nonlinear least-squares fitting routine of the data analysis program Origin (OriginLab, Northampton, MA) using the equation $f(x) = f_{max}/[1 + (x/EC_{50})^{nH}]$, where f is the measured firing frequency, f_{max} the maximum firing frequency, x the concentration tested, EC_{50} the half-maximum effective concentration and n_H the slope factor. Senktide concentration-response experiments were also performed with slices pre-incubated for at least 1 h with drugs previous to the firing frequency measurement.

In experiments aimed to assess the rate of block of the drugs, senktide was first applied for 4 min at 20 min intervals in the absence of the drug being investigated. The perfusion of the drug alone started immediately upon recovery of the effect of senktide. Senktide was then applied again for 4 min at 20 min intervals in the presence of the drug. All salts for ACSF solutions were obtained from Sigma-Aldrich (Basel, Switzerland). Stock solutions of talnetant, osanetant and RO4583298 (10 mmol·L^{-1}) were made in dimethyl sulphoxide (DMSO) and diluted in gassed ACSF to reach a final concentration DMSO never exceeding 0.1%.

In vivo evaluation of RO4583298

Animals and drug treatment

Male and female Mongolian gerbils (Biological Research Laboratories, Füllinsdorf, Switzerland and Charles River, Wilmington, MA, USA), weighing 40–70 g, were used. On arrival, gerbils were housed in groups of four (type III transparent polycarbonate cage, L × W × H, 42 × 26 × 15 cm). Male NMRI mice (20–30 g) supplied by RCC Ltd, Füllinsdorf, Switzerland were used and caged in groups of 10 in type III boxes. Animals were allowed at least 5 days to acclimatize to the housing conditions prior to testing. All animals were kept under a normal light–dark cycle (lights on 06:00–18:00 h) in a temperature (20–22°C) and humidity (55 ± 5%) controlled animal facility, with access to food and water *ad libitum*. All experimental procedures received prior approval from the City of Basel Cantonal Animal Protection Committee based on adherence to Swiss federal and local regulations. RO4583298 was dissolved in vehicle: 0.3% (v/v) Tween-80 in physiological saline (0.9% NaCl) and administered in an injection volume of 10 mL·kg^{-1} body weight orally (p.o.) 120 min prior to testing. GR73632 or senktide was dissolved in 0.1% BSA in water and frozen (–20°C) in aliquots until use, where it was given by direct intracerebroventricular (i.c.v.) injection. Experimentally-naive gerbils and mice were used in each study.

NK_1 agonist-induced foot tapping in gerbil

Gerbils were anaesthetized by inhalation of isoflurane/oxygen mixture, the scalp was exposed and GR73632 (3 pmol

5 μL^{-1}) or vehicle (0.1% BSA) was administered into the lateral ventricles (i.c.v.) via a cuffed 25 gauge needle vertically inserted to a depth of 4.5 mm below bregma. The incision was closed using a clip suture and gerbils were placed into Perspex boxes on recovery of their righting reflex. Duration (s) of foot tapping behaviour over a 5 min period was measured. For the dose-response experiment, RO4583298 (0.3, 1, 3 mg·kg^{-1}, n = 8 gerbils per dose) or vehicle was administered p.o., 120 min prior to the i.c.v. injection of GR73632 (3 pmol 5 μL^{-1}). To determine the duration of *in vivo* activity in the foot tapping experiment, gerbils (n = 8 per time point) were orally administered RO4583298 (1 mg·kg^{-1}) or vehicle followed by i.c.v. injection of GR73632 (3 pmol 5 μL^{-1}) at various times (1, 2, 4, 8, 12, 24, 36 and 48 h) post-administration.

NK_3 agonist-induced tail whips in NMRI mouse

I.c.v. injections of senktide in NMRI mice (similar procedure as previously described) were performed under isoflurane anaesthesia (5% at induction, 2.5% for maintenance) free hand and observations commenced immediately after arousal from anaesthesia (normally 2–3 min following injection). Mice were placed in a perspex box (13 × 23.5 × 14.5 cm) and the number of tail whip bursts (consisting of lateral undulations that induced a rattling sound in the Perspex box) was counted manually for a period of 20 min. The optimal dose of senktide (0.05 nmol in 5 μL i.c.v.) and the number of tail whips (a period of 20 min counting) were selected based on our previous senktide dose-response study in NMRI mice (Nordquist *et al.*, 2010). For the dose-response experiment, RO4583298 (1, 3, 10, 30 mg·kg^{-1} p.o., n = 10 mice per dose) or vehicle was administered 120 min prior to the i.c.v. injection of senktide (0.05 nmol 5 μL^{-1}). To determine the duration of *in vivo* activity in the tail whip experiment, mice (n = 8 per time point) were orally administered RO4583298 (10 mg·kg^{-1}) or vehicle followed by i.c.v. injection of senktide (0.05 nmol 5 μL^{-1}) at various times (1, 2, 4, 8, 24 and 48 h) post-administration.

Pharmacokinetic/pharmacodynamic studies in gerbil and mouse

To determine the plasma exposure of RO4583298 during time course experiments, blood samples were collected from gerbils and mice immediately after *in vivo* testing in gerbil foot tapping and mouse tail whips as described above, placed into microcentrifuge tubes, and then centrifuged to isolate plasma. The plasma samples were frozen (–20°C) until analysis for concentrations. For determination of brain exposure during time course experiments, brain tissues of gerbils and mice at various time points were collected. For sample preparation, 50 μL of plasma was mixed with 150 μL of methanol containing an internal standard. Brain tissue (i.e. one gerbil or one mouse brain) was diluted with three volumes of water and homogenized in an ice-water bath using an ultrasonic probe. Fifty μL of the homogenized brain sample was mixed with 150 μL methanol containing an internal standard. Brain and plasma samples were centrifuged, 100 μL of the upper organic phase was diluted with one volume of water and analysed by liquid chromatography and tandem mass spectrometry (LC/MS/MS).

Data analysis

Unless otherwise noted, results are shown as means ± SEM and significant differences between means were determined using one-way analysis of variance followed post hoc by the Mann–Whitney *U*-test (one tailed). A *P*-value of 0.05 was accepted as statistically significant.

Materials

Aprepitant (MK-869, 2-(R)-(1-(R)-3,5-bis(trifluromethyl) phenylethoxy)-3-(S)-(4-fluoro)phenyl-4-(3-oxo-1,2,4-triazol-5yl)methylmorphine), CP-96 345 ((2S, 3S)-*cis*-2-(diphenylmethyl)-N-[(2-methoxyphenyl)-methyl]-1-azabicyclo[2.2.2]octan-3-amine), GR73632 (H2N-(CH2)4-CO-Phe-Pro-NMe-Leu-Met-NH2), MDL 105 212 (1-{2-[(R)-3-(3,4-dichlorophenyl)-1-(3,4,5-trimethoxy-benzoyl)-pyrrolidin-3-yl]-ethyl}-4-phenyl-piperidine-4-carboxylic acid amide), osanetant (SR142801 (S)-(+)-N-((3-[1-benzoyl-3-(3,4-dichlorophenyl) piperidin-3-yl]prop-1-yl)-4-phenylpiperidin-4-yl)-N-methylacetamine), RO4583298 ((2R,3S)-2-(3,5-bis-trifluoromethyl-phenyl)-N-[4-(4-fluoro-2-methyl-phenyl)-6–(3-hydroxy-2-hydroxymethyl-pyrrolidin-1-yl)-pyridin-3-yl]-N-methyl-isobutyramide), SB222200 ((*S*)-(-)-*N*-(α-ethylbenzyl)-3-methyl-2-phenylquinoline-4-carboxamide), talnetant (SB223412 (*S*)-(-)-*N*-(α-ethylbenzyl)-3-hydroxy-2-phenylquinoline-4-carboxamide) were synthesized within the Chemistry department of F. Hoffmann-La Roche. [^{3}H]-osanetant ([^{3}H]-SR142801, specific activity: 74.0 Ci·mM^{-1}), [^{3}H]-SP ([^{3}H]-substance P, specific activity: 40.0 Ci·mM^{-1}), [^{3}H]-senktide (specific activity: 59.0 Ci·mM^{-1}), [^{3}H]-SR48968 (specific activity: 27.0 Ci·mM^{-1}), [*myo*-1,2-^{3}H]-inositol with PT6-271 (specific activity: 16.0 Ci·mM^{-1}) and yttrium silicate (Ysi) RNA binding beads were purchased from GE Healthcare UK limited, Chalfont St. Giles, UK. [MePhe^7]-Neurokinin B (H-Asp-Met-His-Asp-Phe-Phe-NMe-Phe-Gly-Leu-Met-NH$_2$) was purchased from NeoMPS SA (Strasbourg, France). Substance P and senktide (succinyl-Asp-Phe-Me-Phe-Gly-Leu-Met-NH2) were obtained from Tocris Biosciences (Bristol, UK).

Results

Radioligand binding characteristics of RO4583298 at NK receptors and comparison with selective NK_1 and NK_3 antagonists

RO4583298 (2-phenyl-N-(pyridin-3-yl)-N-methylisobutyramide derivative), which was serendipitously discovered during a programme directed at identifying selective NK_1 antagonists, belongs to a novel structural class binding to both NK_1 and NK_3 (Hoffmann *et al.*, 2005; Peters *et al.*, 2010). Its chemical structure is different from that of selective NK_1 (aprepitant and CP-96 345) and NK_3 (osanetant and talnetant) antagonists (Figure 1). To characterize the *in vitro* binding of RO4583298 at NK receptors from different species, competition radioligand binding was performed using NK specific radioligands [^{3}H]-SP, [^{3}H]-SR48968, [^{3}H]-osanetant or [^{3}H]-senktide and HEK293 cell membranes from transiently expressing NK receptors. In the saturation studies, the specific

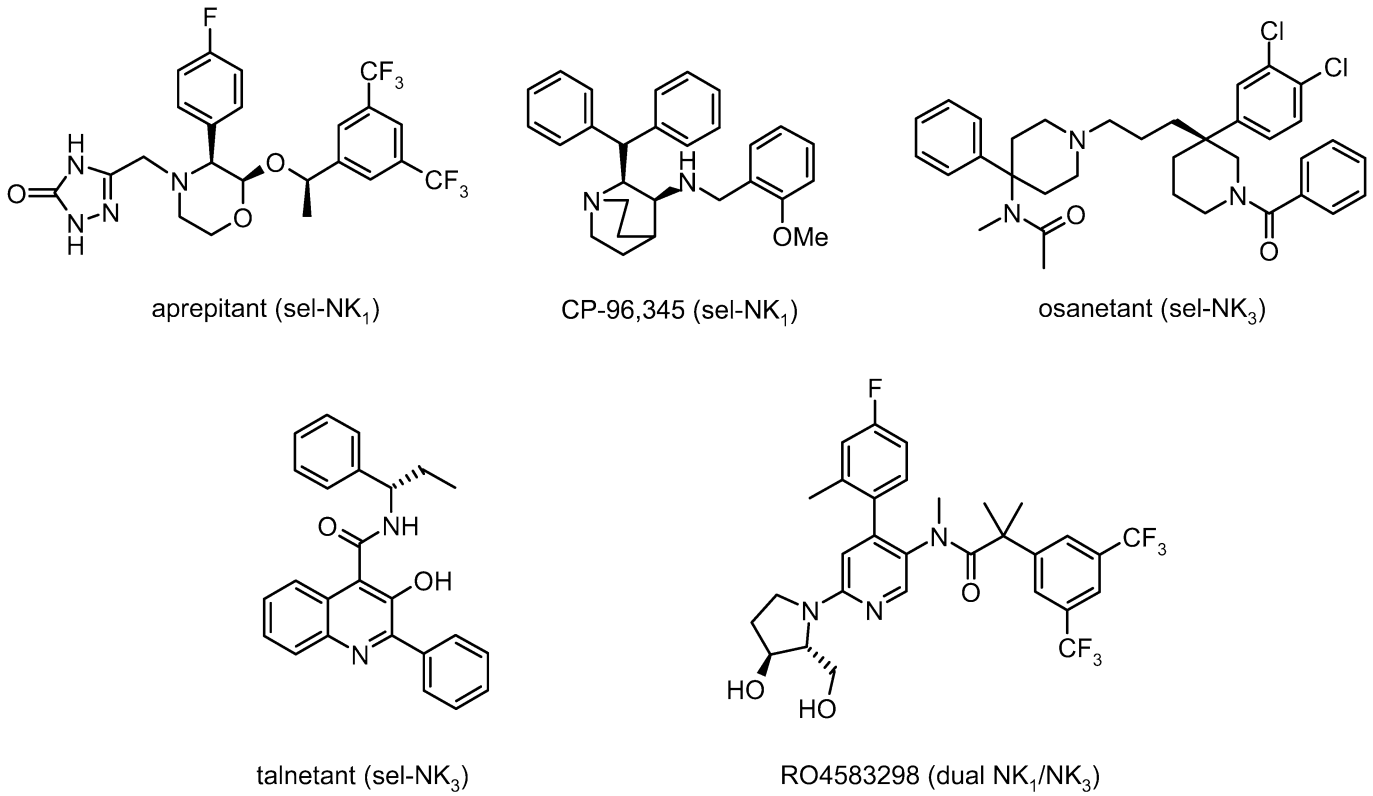

Figure 1

Chemical structures of the selective NK_1, NK_3 and dual NK_1/NK_3 antagonists.

Table 1

Radioligand binding-affinity of NK antagonists in membrane preparations from HEK293 cells transiently expressing hNK_1, gNK_1, or hNK_2

NK antagonists	[^{3}H]SP K_i nmol·L^{-1}	pK_i	n_H	K_i nmol·L^{-1}	pK_i	n_H	[^{3}H]SR48968 K_i nmol·L^{-1}	pK_i	n_H
Aprepitant	0.46 ± 0.0	9.34	1.1 ± 0.0	0.74 ± 0.1	9.13	1.77 ± 0.2	>10 000	<5.0	
CP-96,345	0.41 ± 0.2	9.39	0.53 ± 0.0	0.28 ± 0.1	9.56	0.7 ± 0.1	>10 000	<5.0	
RO4583298	0.72 ± 0.1	9.14	1.0 ± 0.1	0.84 ± 0.2	9.07	1.76 ± 0.2	65.0 ± 7.3	7.19	0.8 ± 0.1

The affinity constant (K_i or pK_i) and Hill slope (n_H) values for various antagonists determined using either [^{3}H]-SP or [^{3}H]-SR48968, were calculated as described in the Methods. Radioligand concentrations: 0.3 and 0.2 nmol·L^{-1} of [^{3}H]-SP for hNK_1 and gNK_1 membranes, respectively; 0.4 nmol·L^{-1} of [^{3}H]-SR48968 for hNK_2 membrane. Values are ±SEM of the K_i calculated from three independent experiments, each performed in duplicate.

binding of [^{3}H]-SP to human and gerbil NK_1 receptors was not saturable. The saturation binding isotherms of [^{3}H]-SP were biphasic and best fitted to a two-side model (Figure 2A,B). [^{3}H]-SP bound on recombinantly expressed hNK_1 and gNK_1 receptors to a high-affinity site (K_{Dhi} of 0.3 and 0.2 nmol·L^{-1}; B_{maxhi} of 26.3 and 2.3 pmol·mg^{-1} protein, respectively) and to a low-affinity site (K_{Dlo} of 87.8 and 7.8 nmol·L^{-1}; B_{maxlo} of 80.5 and 17.4 pmol·mg^{-1} protein, respectively). The competition curves for NK antagonists using a sigmoidal dose-response (variable slope) are shown in Figure 2C,D. RO4583298, as well as aprepitant and CP-96,345, were able to displace the [^{3}H]-SP binding from hNK_1 and gNK_1 membranes with K_i values summarized in Table 1. RO4583298 and aprepitant displayed a Hill slope (n_H) close to unity for hNK_1 membrane, showing no cooperativity was involved in the binding (Table 1). However, both antagonists had a Hill slope greater than 1.0 for gNK_1 membrane, which might point to multiple binding sites with positive cooperativity (Table 1). Interestingly, CP-96 345 yielded shallow binding curves with Hill slopes less than 1.0 for both hNK1 and gNK_1 membranes; this may indicate multiple binding sites with different affinities for ligand or negative cooperativity (Figure 2C,D, Table 1).

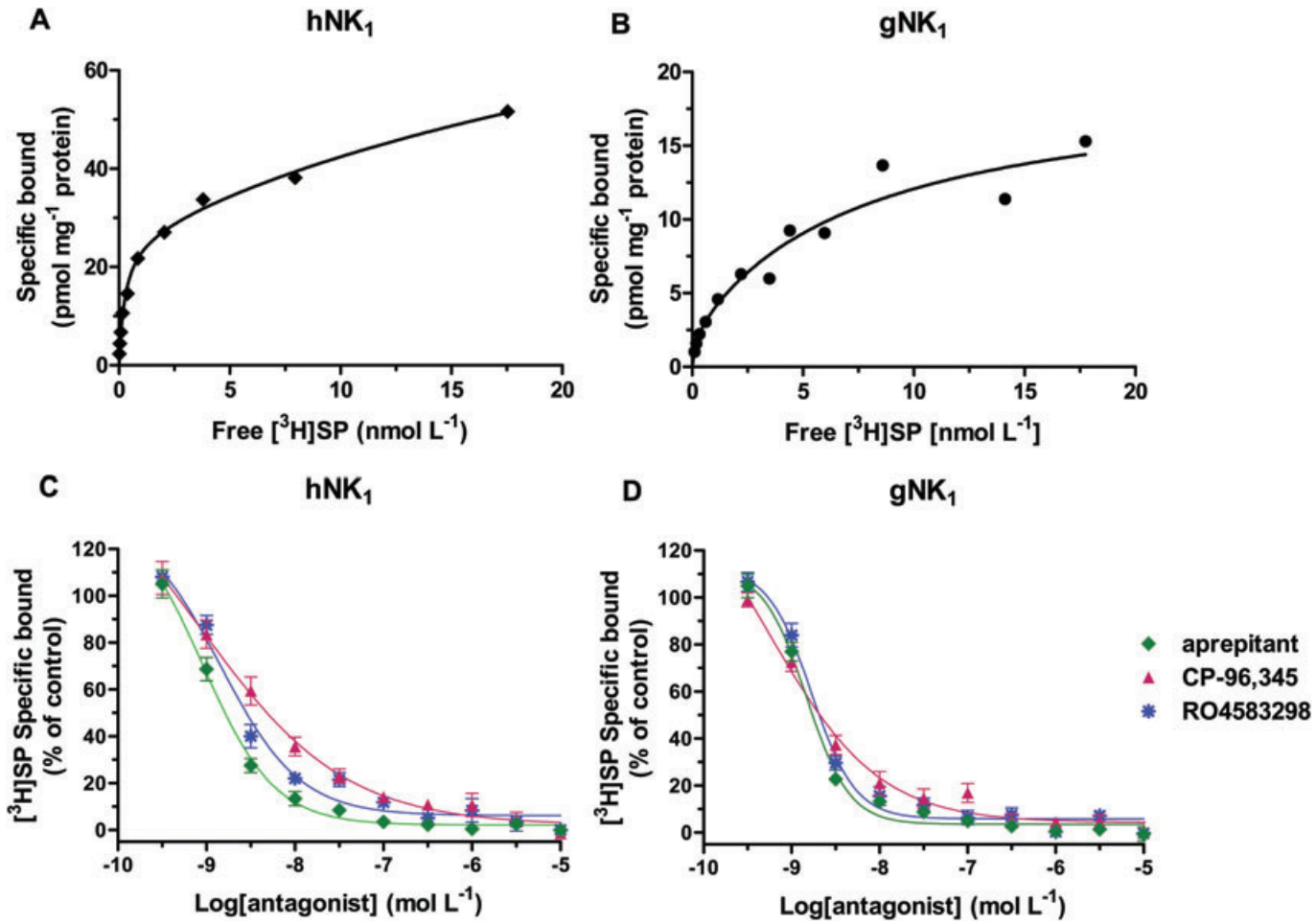

Figure 2

A,B. Saturation binding curves for [^{3}H]-SP binding to membrane from HEK293 cells transfected transiently with hNK_1 or gNK_1, respectively. The data were analysed by nonlinear regression analysis using GraphPad Prism 5.0 software and the two-site binding model. C,D. Binding affinities of selective NK_1 and dual NK_1/NK_3 antagonists for inhibition of [^{3}H]-SP binding to the membrane preparations from HEK293 cells transiently expressing hNK_1 or gNK_1. [^{3}H]-SP was used at a concentration of 0.3 and 0.2 nmol·L^{-1} for hNK_1 and gNK_1 membranes, respectively, in these competition binding experiments. Each data point is mean ± SEM (bars) of three independent experiments performed in duplicate. The data were analysed by a sigmoidal dose-response (variable slope) using GraphPad Prism 5.0 software.

RO4583298 displaced [^{3}H]-SR48968 (K_D and B_{max} of 0.4 ± 0.01 nmol·L^{-1} and 10.0 ± 0.6 pmol·mg^{-1} protein) from hNK_2 membranes with a pK_i of 7.19 (Table 1).

[^{3}H]-osanetant is a selective NK_3 radioligand that binds to a single saturable site on recombinantly expressed hNK_3, $cmNK_3$, gNK_3 and $gpNK_3$ receptors (B_{max} of 8.0 ± 0.3, 19.5 ± 1.8, 18.2 ± 1.1 and 38.5 ± 2.0 pmol·mg^{-1} protein, respectively), with high-affinity (K_D of 0.20 ± 0.01, 0.10 ± 0.0, 0.1 ± 0.0, and 0.15 ± 0.03 nmol·L^{-1}, respectively). As seen in Table 2, RO4583298 and selective NK_3 antagonists strongly inhibited the [^{3}H]-osanetant binding in hNK_3, $cmNK_3$, gNK_3 and $gpNK_3$ membranes. Senktide, which is a synthetic peptide, has previously been shown to be a highly selective and potent agonist at the NK_3 with pK_i values of 8.54, <5.0, and <5.0 at hNK_3, hNK_2 and hNK_1, respectively (Sarau *et al.*, 1997). Because our in-house binding studies indicated a high level of non-specific binding of [^{3}H]-osanetant to mouse and rat NK_3 membranes and because osanetant was previously shown to have a lower affinity for rNK_3 (pK_i of 7.96) in comparison to hNK_3 (pK_i of 9.4) (Chung *et al.*, 1995), in the current study, [^{3}H]-senktide competition binding was used to assess the *in vitro* binding of antagonists at mouse and rat NK_3. In saturation binding analyses, [^{3}H]-senktide binds to a single saturable site on recombinantly expressed mNK_3 and rNK_3 (B_{max} of 0.92 ± 0.01 and 4.5 ± 0.4 pmol·mg^{-1} protein, respectively), with high-affinity (K_D of 2.6 ± 0.2, and 3.0 ± 0.5 nmol·L^{-1}, respectively). The affinity constants of RO4583298 and selective NK_3 antagonists in membrane preparations from HEK293 cells transiently expressing mNK_3, or rNK_3 are given in Table 2. Consistent with previous reports (Chung *et al.*, 1995; Emonds-Alt *et al.*, 1995; Sarau *et al.*, 1997; 2001), we also observed decreases in binding-affinity for talnetant and osanetant at mNK_3 and rNK_3, respectively, in comparison to hNK_3. However, RO4583298 displayed a

Table 2

Radioligand binding-affinity of NK antagonists in membrane preparations from HEK293 cells transiently expressing NK_3 receptors from different species

	NK_3 receptor	Talnetant K_i nmol·L^{-1}	pK_i	n_H	Osanetant K_i nmol·L^{-1}	pK_i	n_H	RO4583298 K_i nmol·L^{-1}	pK_i	n_H
[^{3}H]osanetant	Human	3.0 ± 0.4	8.52	0.9 ± 0.1	0.5 ± 0.0	9.3	1.0 ± 0.0	2.9 ± 0.3	8.54	1.1 ± 0.1
	Cynomolgus monkey	3.2 ± 0.5	8.49	0.8 ± 0.1	0.8 ± 0.0	9.10	1.1 ± 0.0	1.1 ± 0.3	8.96	1.3 ± 0.0
	Gerbil	1.2 ± 0.3	8.92	0.9 ± 0.1	0.8 ± 0.1	9.10	1.2 ± 0.2	2.0 ± 0.6	8.70	0.9 ± 0.1
	Guinea pig	5.0 ± 1.5	8.30	1.0 ± 0.1	0.6 ± 0.2	9.22	1.0 ± 0.1	5.3 ± 1.0	8.28	1.2 ± 0.0
[^{3}H]senktide	Mouse	68.0 ± 3.4	7.17	1.0 ± 0.0	31.1 ± 1.4	7.51	0.9 ± 0.1	5.0 ± 0.8	8.3	1.0 ± 0.1
	Rat	85.6 ± 11.4	7.07	0.8 ± 0.1	23.0 ± 5.0	7.64	0.8 ± 0.1	3.6 ± 0.8	8.44	1.0 ± 0.1

The affinity constant (K_i or pK_i) and Hill slope (n_H) values for the various antagonists were determined using either [^{3}H]-osenetant or [^{3}H]-senktide, were calculated as described in the Methods. Radioligand concentrations: 0.2, 0.1, 0.1 and 0.15 nmol·L^{-1}of [^{3}H]-osanetant for hNK_3, $cmNK_3$, gNK_3 and $gpNK_3$ membranes, respectively; 2.6 and 3.0 nmol·L^{-1} of [^{3}H]-senktide for mNK_3 and rNK_3 membranes, respectively. Values are ±SEM of the K_i calculated from three independent experiments, each performed in duplicate. K_i values for talnetant and osanetant at hNK_3 and $gpNK_3$ are taken from Malherbe *et al.* (2009) and are shown here for comparison.

similar binding-affinity at NK_3 receptors from various species including mouse and rat (Table 2).

The pharmacological specificity of RO4583298 was confirmed by testing it in radioligand binding assays in a broad CEREP screen (Paris, France, www.cerep.fr) at concentrations of 0.1 and 10 µmol·L^{-1}. Among the 64 receptors in the CEREP broad screen, 23 were peptide GPCR receptors. At 0.1 µmol·L^{-1}, RO4583298 was completely inactive at all targets tested. At 10 µmol·L^{-1}, it displayed activity at Ca^{2+} L channel (DHP site) and Na^+ channel, where it caused 96% and 99.4%, respectively, displacement of specific binding. However, subsequent electrophysiological recordings of RO4583298 in cells expressing human Na^+ channel or rat Ca^{2+} L channel showed IC_{50} values of 3.4 and 11 µmol·L^{-1}, respectively. It should be noted that these concentrations are >4700- and >1200-fold higher than RO4583298's affinity for the hNK_1 and hNK_3.

Inhibition mode of RO4583298 on the SP- or [MePhe^7]NKB-evoked accumulation of [^{3}H]-IP at various NK receptor species

To compare the inhibition mode of RO4583298 and selective NK_1 and NK_3 antagonists for different NK species, the concentration-response curves (CRCs) for [^{3}H]-IP formation stimulated by SP or [MePhe^7]NKB were measured in the absence or presence of increasing concentrations of antagonist in the HEK293 cells transiently transfected with various NK receptors. In the hNK_1 or gNK_1 expressing cells, SP (NK_1-agonist that binds with pKi of 8.55, 6.89 and 5.89 to hNK_1, hNK_2 and hNK_3, respectively) elicited concentration-dependent increases in the accumulation of [^{3}H]-IP with EC_{50} values of 0.6 ± 0.0 and 0.5 ± 0.0 nmol·L^{-1}, respectively. Consistent with a previous report (Hale *et al.*, 1998), aprepitant (a selective NK_1 antagonist) displayed an apparent non-competitive mode of antagonism at both hNK_1 and gNK_1, shifting SP CRCs to the right with a concomitant decrease in maximal response. Whereas CP-96 345 (selective NK_1 antagonist) (Lowe *et al.*, 1992) behaved as a competitive antagonist at both hNK_1 and gNK_1 shifting the SP CRCs to the right without changing its maximal response (pA_2 of 8.27 and 8.44; Schild slope of 1.19 and 0.98, respectively). RO4583298 also behaved as a non-competitive antagonist at both hNK_1 and gNK_1 producing a rightward shift in SP CRC as well as a full suppression of the maximal response (Figure 3A,B).

[MePhe^7]NKB was used as an agonist, because it has been shown to have a high selectivity for hNK_3 (pK_i of 9.52) versus hNK_2 (pK_i of 5.80) and hNK_1 (pK_i <5) (Sarau *et al.*, 1997). [MePhe^7]NKB elicited concentration-dependent increases in the accumulation of [^{3}H]-IP in HEK293 cells expressing the hNK_3, $cmNK_3$, gNK_3, $gpNK_3$, mNK_3 or rNK_3 with the EC_{50} values of 0.6 ± 0.0, 0.89 ± 0.04, 0.27 ± 0.01, 0.6 ± 0.0, 0.31 ± 0.01 and 0.26 ± 0.05 nmol·L^{-1}, respectively. RO4583298 displayed a non-competitive mode of antagonism at hNK_3, $cmNK_3$, gNK_3, $gpNK_3$ receptors (Figure 4A–D; Table 3), but it behaved in a partial non-competitive manner at mNK_3 and rNK_3 (Figure 5A,B; Table 3). The maximal [MePhe^7]NKB-evoked response was depressed by 74%, 81%, 56%, 76%, 10%, 29% of the control response (NKB-alone) in the presence of 100 nmol·L^{-1} of RO4583298 at hNK_3, $cmNK_3$, gNK_3, $gpNK_3$, mNK_3 or rNK_3, respectively. Both talnetant and osanetant behaved as competitive antagonists at hNK_3, $cmNK_3$, gNK_3, mNK_3 or rNK_3 shifting the NKB CRC to the right without changing its maximal response (Figures 4E,F, 5C–F; pA_2 and slope values shown in Table 3). As we have previously reported, osanetant had an apparent non-competitive mode of antagonism at $gpNK_3$ while talnetant was competitive (Malherbe *et al.*, 2009). The NK transfected HEK293 cells exhibited some basal activity (~600 CPM) in comparison to mock transfected (~200 CPM), this basal activity decreased by <5% in the presence of 100 nmol·L^{-1} RO4583298. Since in a physiologically native system such as midbrain slices, RO4583298 (100 nmol·L^{-1}) alone did not exhibit any effect on the firing rate of the DA neurones of SNpc, a high expression level of NK receptors in the transfected HEK293 cells has to be responsible for the basal activity.

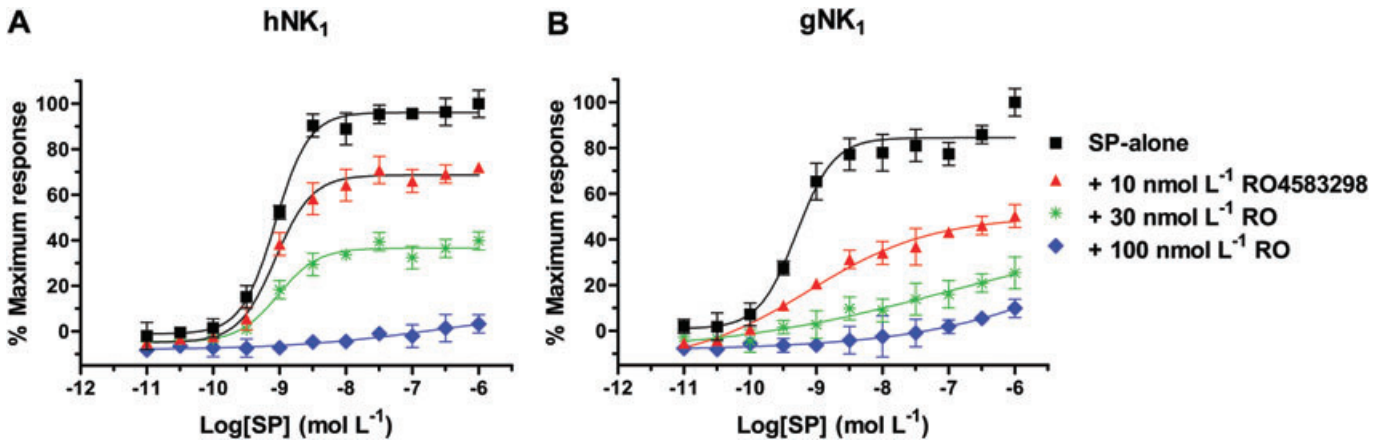

Figure 3

Schild analyses showing the non-competitive-like mode of antagonism by RO4583298 at hNK_1 and gNK_1. Concentration-response curves (CRCs) for [^{3}H]-IP formation stimulated by SP in the absence or presence of increasing concentrations of RO4583298 (A and B) in HEK293 cells expressing transiently the hNK_1 or gNK_1. Each point represents mean ± SEM (bars) of six measurements from three independent transfections. Cells were incubated with antagonists for 20 min at 37°C prior to stimulation with SP.

Effect of talnetant, osanetant and RO4583298 on senktide-induced increase of spontaneous activity of dopaminergic neurones

Previous *in vitro* electrophysiological recordings in guinea-pig midbrain slices have demonstrated that the selective NK_3 agonist senktide increases the firing frequency of dopaminergic (DA) SNpc neurones. This effect was inhibited by the selective NK_3 antagonist SR 142801 (osanetant), whereas its S-enantiomer SR 142806 and selective antagonists of NK_1 (SR 140333) or NK_2 (SR 48968) receptors were completely inactive (Nalivaiko *et al.*, 1997). In the current study, we have used this electrophysiological paradigm to compare the antagonistic effect of RO4583298 with that of the selective NK_3 antagonists talnetant and osanetant. In control slices, senktide concentration-dependently increased the firing frequency of DA SNpc neurones (Figure 6A,C). The Max, pEC_{50} and Hill values for senktide-induced increase of firing frequency were 182 ± 9.2%, 8.7 ± 0.1 and 1.0 ± 0.1 (n = 11), respectively. In contrast, in slices incubated with 100 nmol·L^{-1} RO4583298 for at least one hour, senktide did not increase the firing frequency of the DA neurones at all concentrations tested (n = 7; Figure 6B,C). This suggests a non-competitive mechanism of action of RO4583298. In slices incubated for a least 1 h with 100 nmol·L^{-1} talnetant, senktide concentration-dependently increased the firing frequency of DA neurones with Max, pEC_{50} and Hill values of 167 ± 17%, 7.5 ± 0.1 and 1.5 ± 0.2 (n = 4), respectively (Figure 6C). The senktide concentration-response curve in the presence of talnetant was therefore shifted to the right; however, the maximum increases of firing frequency in the absence and presence of talnetant were comparable. This suggests a competitive mechanism of action of talenant. The apparent pA_2 value for talnetant was 8.22. These results are in good agreement with a previous report that talnetant antagonized senktide-induced increases in neuronal firing in the SNpc with pA_2 value of 7.7 and with a competitive mode of antagonism (Dawson *et al.*, 2008). In another set of experiments, senktide (10 nmol·L^{-1}) was applied to spontaneously active DA neurones for 4 min at 20 min intervals in the absence or presence of osanetant, talnetant and RO4583298. As shown in Figure 7 for three representative DA neurones, the compounds had no detectable effect on spontaneous activity. Whilst osanetant (1 μmol·L^{-1}) inhibited the senktide-induced increase only partially after five applications of senktide in the presence of osanetant (Figure 7A), full inhibition of the senktide effect was observed after two and three applications of senktide in the presence of talnetant (100 nmol·L^{-1}) and RO4583298 (1 μmol·L^{-1}), respectively (Figure 7B,C).

In vivo activity of RO4583298

Effect of RO4583298 on NK_1 agonist (GR73632)-induced foot tapping behaviour in gerbil

As we have previously shown (Ballard *et al.*, 2001), injection of 3 pmol 5 μL^{-1}, i.c.v. of a potent, selective NK_1 agonist, GR73632 (pEC_{50} of 8.70 at hNK_1 versus pEC_{50} of <5.0 and <5.0 at hNK_2 and hNK_3), produced foot tapping behaviour in gerbils (n = 8), with a cumulative score of 297.60 ± 1.03 s during a 5 min test session. This behaviour was significantly blocked in a dose-dependent manner by pretreatment (2 h) with the dual NK_1/NK_3 antagonist, RO4583298 (Mann–Whitney U-test, P < 0.01) at 1 and 3 mg·kg^{-1} p.o and had an ED_{50} of 0.4 mg·kg^{-1} (Figure 8A). When administered alone, RO4583298 did not induce any foot tapping behaviour. The time course of the inhibitory effect of RO4583298 (1 mg·kg^{-1}, p.o.) is shown in Figure 8B. RO4583298 had a $t_{1/2}$ of 14 h.

Effect of RO4583298 on NK_3 agonist (senktide)-induced tail whips in mice

As we have previously shown (Nordquist *et al.*, 2010), shortly after i.c.v. injection of senktide at a dose of 0.05 nmol 5 μL^{-1}, the mice exhibited bursts/bouts of tail whips within a 20 min

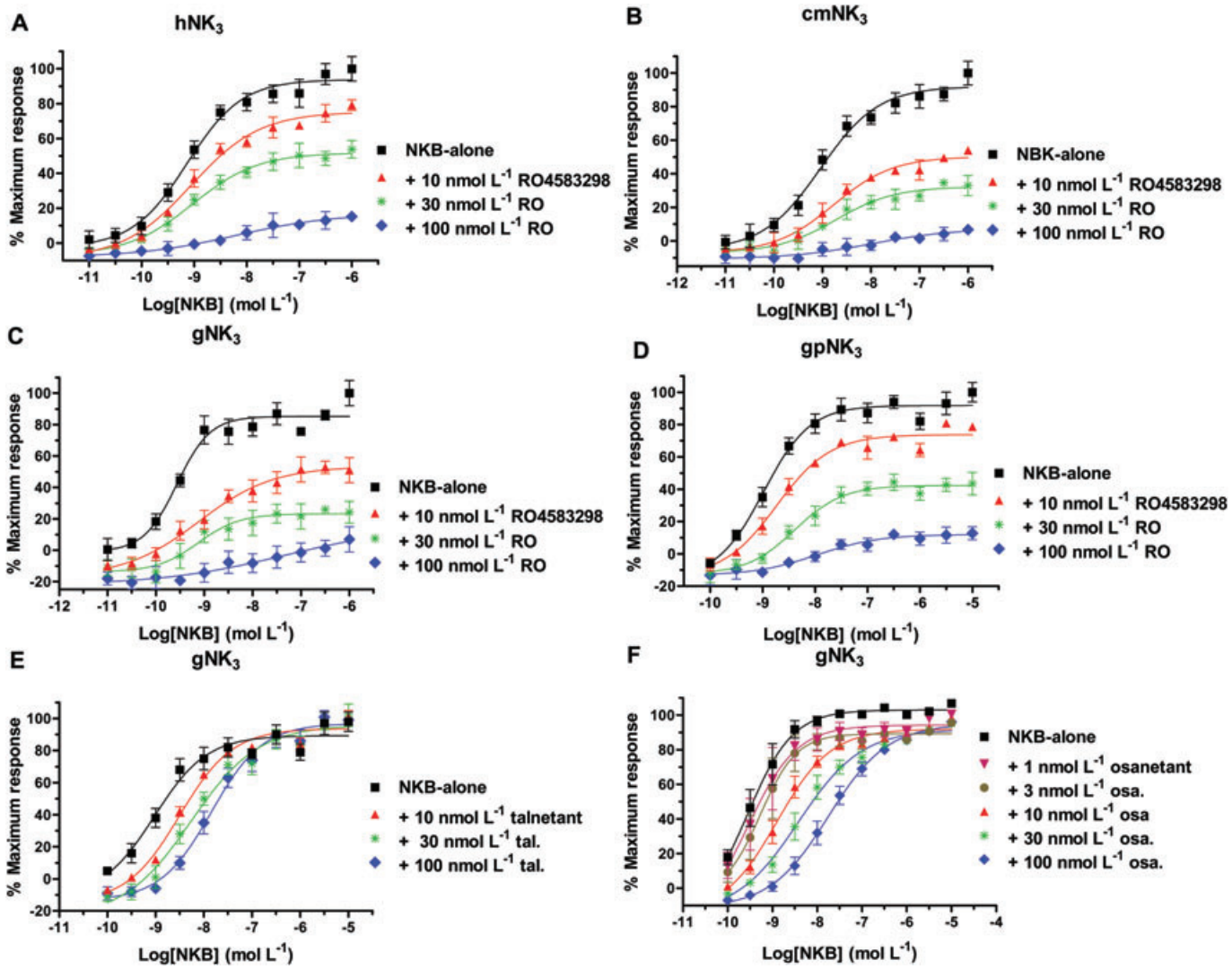

Figure 4

Schild analyses showing the non-competitive like mode of antagonism by RO4583298 at hNK_3, $cmNK_3$, gNK_3 and $gpNK_3$, and competitive antagonism by talnetant and osanetant at gNK_3. Concentration-response curves (CRCs) for [^{3}H]-IP formation stimulated by [MePhe^7]NKB in the absence or presence of increasing concentrations of RO4583298 (A, B, C and D), talnetant (E) or osanetant (F) in HEK293 cells expressing transiently the hNK_3, $cmNK_3$, gNK_3 or $gpNK_3$. Each point represents mean ± SEM (bars) of six measurements from three independent transfections. Cells were incubated with antagonists for 20 min at 37°C prior to stimulation with [MePhe^7]NKB.

period. Oral administration of RO4583298 (2 h pretreatment) produced a dose-dependent inhibition of senktide-induced tail whips (Figure 9A), which was significant at 10 and 30 mg·kg^{-1} (Mann–Whitney *U*-test, $P < 0.01$) and had an ED_{50} of 9.0 mg·kg^{-1}. When administered alone, RO4583298 did not induce any burst of tail whip behaviour in mice. Figure 9B shows the duration of inhibition of senktide-induced tail whips by RO4583298 (10 mg·kg^{-1}, p.o.), which had a $t_{1/2}$ of 5 h.

Correlation between RO4583298 plasma exposure and duration of in vivo *inhibitory effect in gerbil and mouse*

To explore the correlation between the plasma concentration of RO4583298 and its *in vivo* efficacy, blood samples were collected at various time points immediately after *in vivo* testing (foot tapping or tail whip assays) from gerbils (administered either 1 or 2 mg·kg^{-1} of RO4583298, p.o. + 3 pmol 5 µL^{-1} of GR73632, i.c.v.; n = 4–8 gerbils per group) and from mice (administered 10 mg·kg^{-1} of RO4583298, p.o. + 0.05 nmol 5 µL^{-1} of senktide, i.c.v.; n = 5–8 mice per group) and the plasma concentrations of RO4583298 were quantified as described earlier. The pharmacokinetic/pharmacodynamic experiments revealed a correlation between the plasma concentration of RO4583298 and its inhibitory effect on GR73632-induced gerbil foot tapping and senktide-induced mouse tail whip behaviours (Figure 10A). The therapeutically active concentration (TAC), which is the plasma concentration of RO4583298 that is observed to have activity in an animal model *in vivo*, was determined from Figure 10A. It might predict the targeted therapeutic active concentration in human.

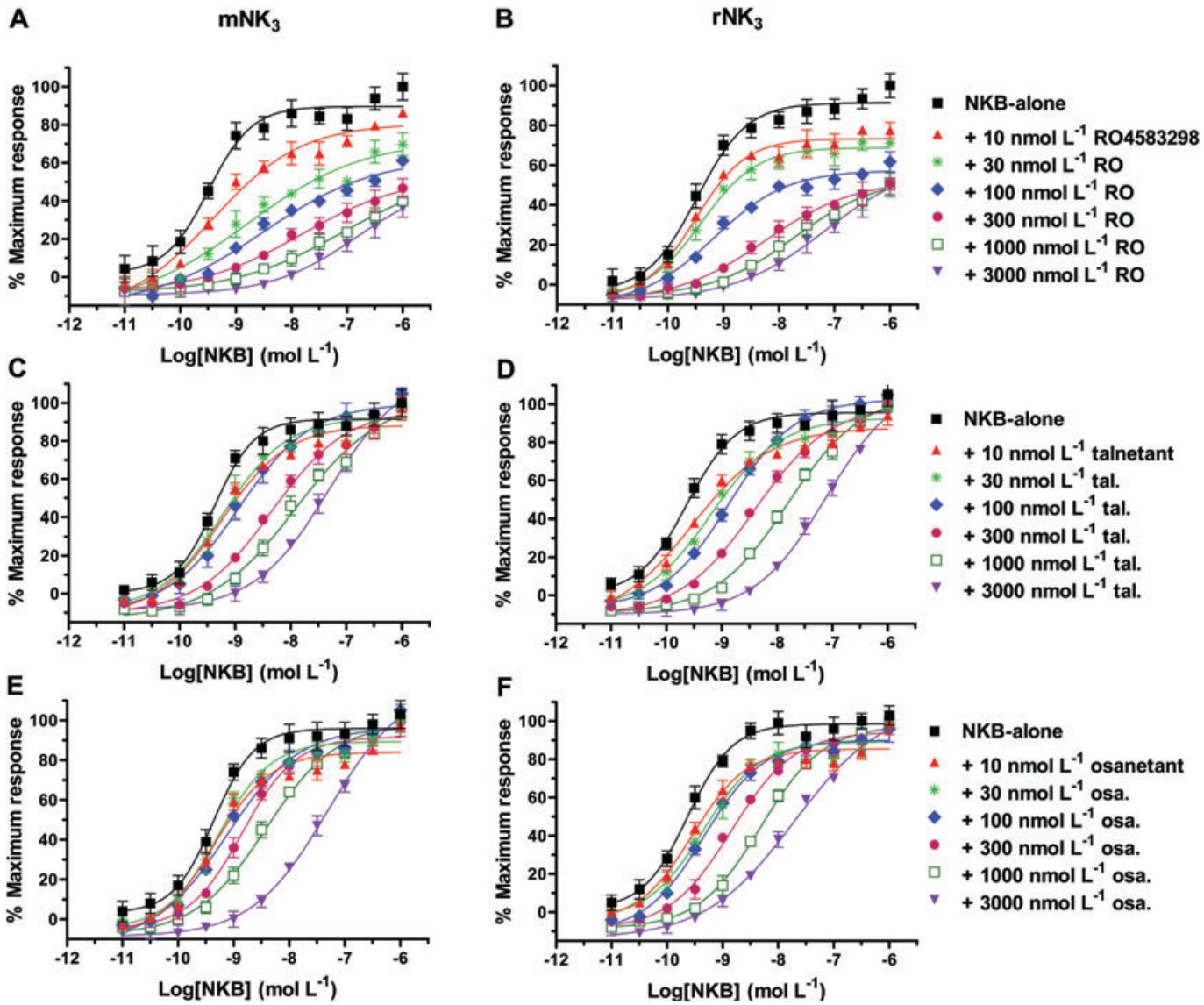

Figure 5

Schild analyses showing the partial non-competitive mode of antagonism by RO4583298, and competitive one by talnetant and osanetant at mouse and rat NK_3 receptors. CRCs for [^{3}H]-IP formation stimulated by [MePhe^7]NKB in the absence or presence of increasing concentrations of RO4583298 (A and B), talnetant (C and D) or osanetant (E and F) in HEK293 cells expressing transiently the mNK_3 and rNK_3 receptors. Each point represents mean ± SEM (bars) of six measurements from three independent transfections. Cells were incubated with antagonists for 20 min at 37°C prior to stimulation with [MePhe^7]NKB.

To determine brain/plasma ratios of RO4583298 during gerbil foot tapping and mouse tail whip time course experiments, brain and plasma concentrations were measured at time points 0.5, 1, 2 and 4 h post-administration of RO4583298 (2 mg·kg^{-1} GFT and 10 mg·kg^{-1} MTW). Figure 10B shows the brain/plasma ratios during GFT and MWT time course studies.

Discussion

Schizophrenia is a major mental disorder that affects 1% of the general population. It is characterized by positive (delusions, hallucinations and paranoia), negative (anhedonia, social withdrawal and self-neglect) and mood (anxiety, dysphoria and suicidality) symptoms, as well as cognitive impairment (memory and attention deficits) (Tamminga and Holcomb, 2005). Current therapies, mainly based on antagonizing D_2/5-HT_{2A} receptors, are largely effective against positive symptoms, but with limited efficacy in the treatment of negative and cognitive symptoms. These treatments also suffer from several side effects including weight gain, diabetes and extrapyramidal symptoms (Leucht *et al.*, 2003). Clinical results of osanetant and talnetant in schizophrenia patients have suggested significant improvement in psychopathology, including positive symptoms with improved efficacy, but

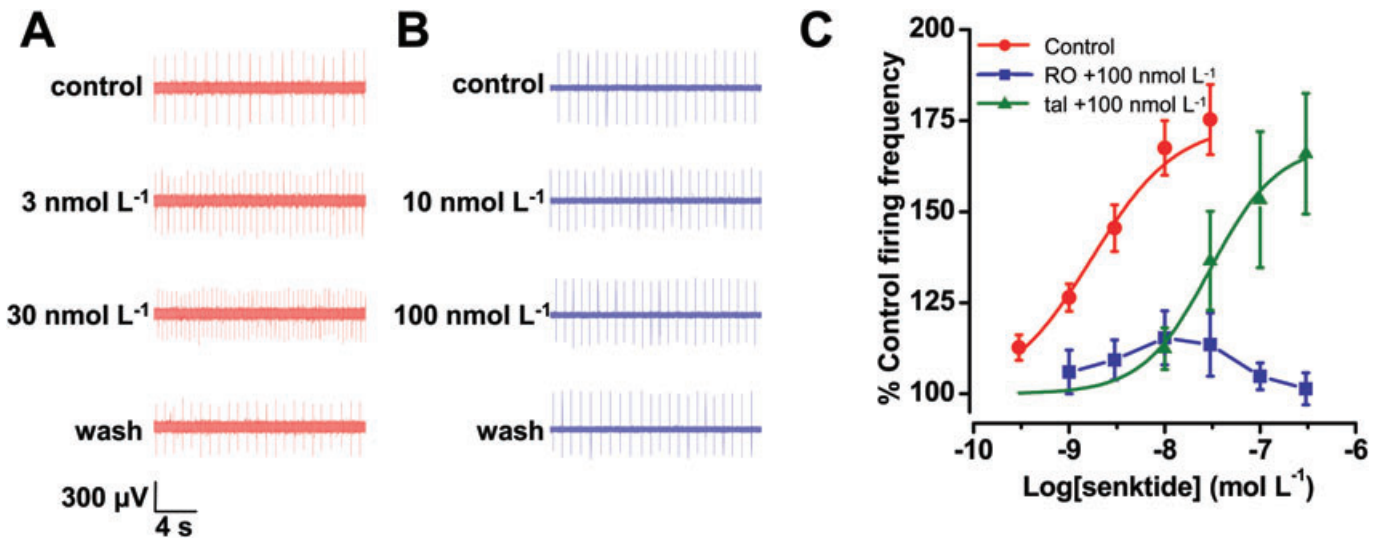

Figure 6

RO4583298 and talnetant differently antagonize the senktide-induced increase in spontaneous firing frequency of dopaminergic neurones from SNpc of guinea-pigs. Representative single unit, spontaneous action potentials recorded extracellularly in the absence and presence of the indicated concentrations of senktide (red traces, A). The same experiment was performed with a different slice pre-incubated for an hour with RO4583298 (100 nmol·L^{-1}; blue traces; B). C. Concentration-response curves for increase of firing frequency induced by senktide in the absence and presence of 100 nmol·L^{-1} RO4583298 or 100 nmol·L^{-1} talnetant, pre-incubated for at least an hour. The points represent the mean ± SEM (bars) of 4–11 neurones from different slices and animals. The sigmoidal curves are fits through these points.

with a lower propensity to induce side effects (Meltzer *et al.*, 2004; Spooren *et al.*, 2005; Meltzer and Prus, 2006). Thus, NK_3 antagonism may offer an alternative therapeutic approach for the treatment of schizophrenia and possibly other psychoses. Here, we describe the *in vitro* and *in vivo* properties of a potent dual NK_1/NK_3 antagonist, RO4583298.

In vitro, RO4583298 exhibits a high-affinity for human and gerbil NK_1 receptors with pK_i 9.14 and 9.07, respectively, as determined using [^{3}H]-SP radioligand binding. Notably, it binds with similar binding-affinity to NK_3 receptors from various species including human, cynomolgus monkey, gerbil, guinea-pig, mouse and rat (pK_i 8.54, 8.96, 8.70, 8.28, 8.30 and 8.44, respectively). RO4583298 has 90- and 22-fold selectivity in binding for hNK_1 and hNK_3 over hNK_2, respectively. Moreover, RO4583298 was assessed over a battery of 64 different binding sites that included numerous other GPCRs, transporters and ion channels. The results obtained indicate that RO4583298 displays a high degree of selectivity for the NK_1/NK_3. Species-related differences in the pharmacology of selective NK_3 antagonists have been reported, especially between human and mouse/rat NK_3: osanetant and talnetant displayed a 28- and 30-fold lower binding-affinity for rat versus human NK_3, respectively, using [^{125}I]-[MePhe^7]NKB binding (Chung *et al.*, 1995; Sarau *et al.*, 1997). In good agreement with these studies, we have similarly observed lower binding-affinity of rat (46- and 28-fold) and mouse (62- and 23-fold) versus human NK_3 for osanetant and talnetant, respectively, using [^{3}H]-senktide competition binding. In this context, two residues in TM2, Met134 and Ala146 of hNK_3 that correspond to Val121 and Gly133 of rat have been demonstrated to be involved in the species-selectivity of SR48968 and osanetant for hNK_3 (Wu *et al.*, 1994; Chung *et al.*, 1995). Furthermore, in the mapping of the binding pocket of osanetant and talnetant to hNK_3, the residue Met134 was also identified as a critical amino acid for both antagonists' binding sites, since the mutation hNK_3-M134A completely abolished the binding-affinity and potency of osanetant and Me-talnetant (Malherbe *et al.*, 2008). Surprisingly, RO4583298 did not show any species-selectivity at rat/mouse NK_3; therefore, two TM2 residues Val121 and Gly133 of rat seemed not to be crucial for the binding pocket of RO4583298. As a whole, these data suggest that RO4583298 is a more universal tool for probing the effects of NK_3 receptors allowing the use of rats and mice.

Investigation of the antagonistic mechanism of RO4583298 revealed that it acts as an apparent non-competitive (pseudo-irreversible) antagonist at both NK_1 (human and gerbil) and NK_3 (human, cynomolgus monkey, gerbil, guinea-pig) receptors. This mode of action was characterized by a parallel rightward shift of the SP or [MePhe^7]NKB concentration-response curves (increase in EC_{50} values) in the presence of increasing RO4583298 concentrations with a concomitant large decrease in the maximal agonist-evoked response (E_{max}). However, RO4583298 displayed a tendency toward a partial non-competitive like mode of antagonism at rat and mouse NK_3 receptors. In this mode of antagonism, an increase of RO4583298 concentration first depressed the maximal response to a limit, and then only produced parallel rightward shifts of the [MePhe^7]NKB concentration-response curves. We have also compared the mode of antagonism of RO4583298 with selective NK_1 (aprepitant and CP-96 345) and NK_3 (osanetant and talnetant) receptor antagonists. Similarly, aprepitant behaved in a non-competitive manner at both human and gerbil NK_1, whereas CP-96 345 acted as a competitive antagonist at both receptors. It had been previously shown that aprepitant had

Table 3

Schild analyses for antagonism of [MePhe^7]NKB-induced accumulation of [^{3}H]-IP by NK antagonists in the HEK293 cells transiently expressing NK_3 receptors from different species

NK_3 receptor	Talnetant pA_2	Talnetant K_b[a] (nmol·L^{-1})	Talnetant Schild slope	Talnetant Mode of antagonism	Osanetant pA_2	Osanetant K_b[a] (nmol·L^{-1})	Osanetant Schild slope	Osanetant Mode of antagonism	RO4583298 Mode of antagonism	% decline in NKB E_{max} (100 nmol·L^{-1} RO)
Human	8.24	5.75	0.88	Competitive	7.73	18.62	1.59	Competitive	Non-competitive	74.0
Cynomolgus monkey	8.49	3.24	1.26	Competitive	8.40	3.98	0.97	Competitive	Non-competitive	81.3
Gerbil	8.44	3.63	0.78	Competitive	8.56	2.75	1.10	Competitive	Non-competitive	56.0
Guinea pig	7.81	15.49	1.07	Competitive				Non-competitive	Non-competitive	76.0
Mouse	7.23	58.88	1.12	Competitive	6.89	128.83	1.29	Competitive	Partial non-competitive	10.0
Rat	7.54	28.84	1.21	Competitive	7.27	53.70	1.01	Competitive	Partial non-competitive	29.0

The apparent antagonist potency (pA_2 or K_b[a]) and Schild slope values were determined from Schild plot analyses. The Schild constant data for talnetant and osanetant for hNK_3 and $gpNK_3$ are taken from Malherbe *et al.* (2009) and are shown here for comparison. Antagonists were incubated for 20 min at 37°C prior to stimulation with [MePhe^7]NKB.

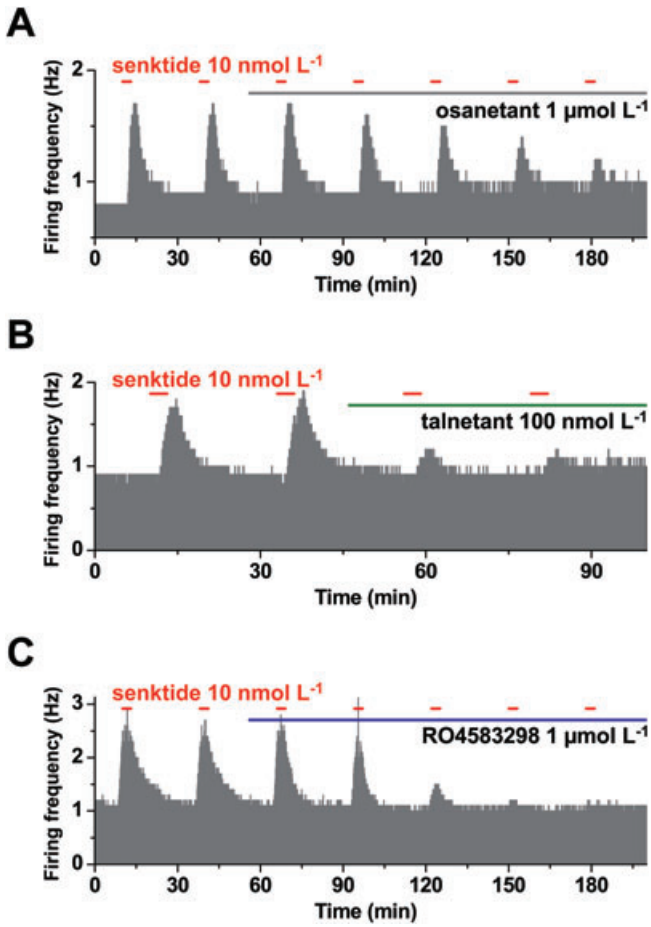

Figure 7

Time course of the antagonistic effect of osanetant, talnetant and RO4583298 on the senktide-induced increase of firing frequency of representative dopaminergic neurones from SNpc of guinea-pigs. Single unit, spontaneous action potentials were recorded extracellularly in the absence and presence of senktide and an NK_3 antagonist. Average firing frequencies were calculated over 1 min intervals and are plotted as a function of time. The short red bars indicate the duration of multiple bath applications of 10 nmol·L^{-1} senktide. Note that the firing frequencies returned to base line upon removal of senktide. The long gray, green, blue bars indicate the duration of bath application of the drugs; osanetant (1 µmol·L^{-1}, A), talnetant (100 nmol·L^{-1}, B) and RO4583298 (1 µmol·L^{-1}, C), respectively.

a very slow rate of dissociation from the hNK_1 receptor ($t_{1/2}$ value of 154 min) and behaved in a pseudo-irreversible or non-competitive manner (Hale *et al.*, 1998; Lindstrom *et al.*, 2007). The apparent non-competitive behaviour of aprepitant was explained by its slow dissociation rate from the receptor. Because of aprepitant's slow dissociation, a large portion of the NK_1 receptor is not available for activation by SP, consequently, the maximally achievable response of SP drops dramatically in comparison to a fast dissociating antagonist such as CP-96 345. With the exception of osanetant, which had an apparent non-competitive behaviour at $gpNK_3$, osanetant and talnetant acted competitively at NK_3 receptors from all other species. As reported previously (Malherbe *et al.*, 2009), TM2 residue Alanine-114 in $gpNK_3$

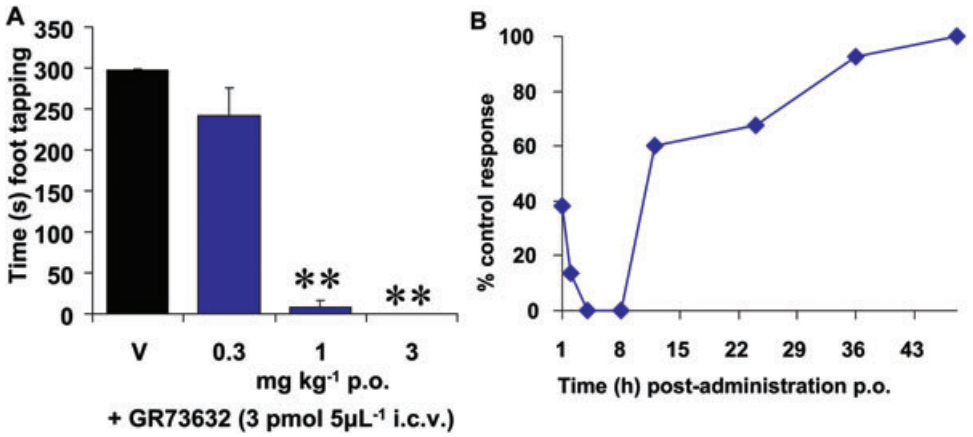

Figure 8

A. Effects of dual NK_1/NK_3 antagonist RO4583298 on NK_1 agonist GR73632-induced foot tapping behaviour in the gerbil. Dose of RO4583298 (p.o.) is indicated on the *x*-axis, time (s) spent foot tapping per 5 min are indicated on the *y*-axis. The pretreatment time was 2 h and $n = 8$ gerbils per dose. B. The duration of inhibitory activity of RO4583298 (1 mg·kg^{-1}, p.o.) on GR73632-induced foot tapping behaviour in the gerbils ($n =$ 8 gerbils per time point) is presented as percentage of control foot tapping (vehicle + GR73632). GR73632 dose is 3 pmol 5 µL^{-1} (i.c.v.) for all groups. Data are presented as mean ± SEM. $^{**}P < 0.01$ compared to vehicle in Mann–Whitney *U*-test.

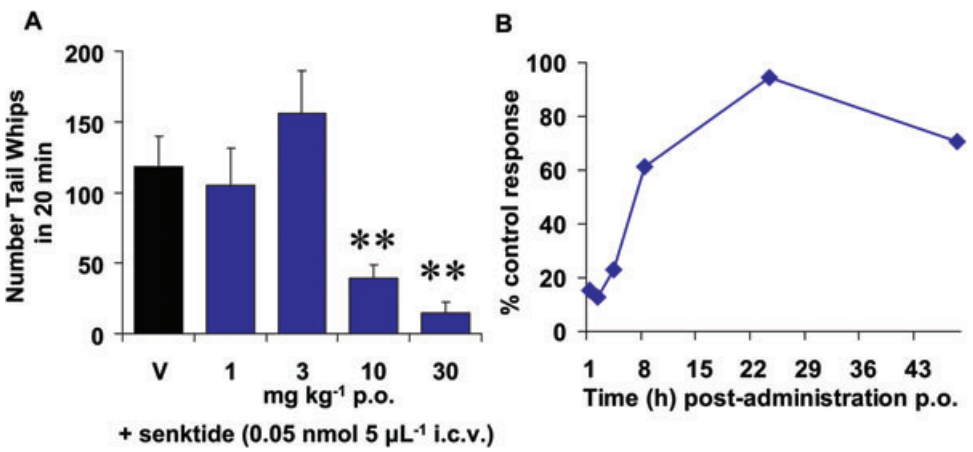

Figure 9

A. Inhibition of NK_3 agonist senktide-induced tail whips by dual NK_1/NK_3 antagonist RO4583298. Dose of RO4583298 (p.o.) is indicated on the *x*-axis, bouts of tail whips are indicated on the *y*-axis. The pretreatment time was 2 h and $n = 10$ mice per dose. B. The duration of inhibitory activity of RO4583298 (10 mg·kg^{-1}, p.o.) on senktide-induced tail whip behaviours in the mice ($n = 8$ mice per time point) is presented as percentage of control tail whips (vehicle + senktide). Senktide dose is 0.05 nmol 5 µL^{-1} (i.c.v.) for all groups. Data are presented as mean ± SEM. $^{**}P < 0.01$ compared to vehicle in Mann–Whitney *U*-test.

(threonine in all other species) was involved in osanetant's apparent non-competitive behaviour by slowing down its dissociation kinetics. Based on our in-house mapping of the binding pocket of RO4583298 to hNK_1 and hNK_3, using molecular modelling and site-directed mutagenesis (unpublished data), we speculate that the very slow dissociation rates of RO4583298 from NK_1 and NK_3 receptors (but not an allosteric site) probably contributes to the apparent non-competitive mode of antagonism, a behaviour very similar to that of aprepitant. Both NK_1 and NK_3 couple to phospholipase C-β and undergo agonist-induced endocytosis and recycling (Grady *et al.*, 1995; Jenkinson *et al.*, 2000; Schmidlin *et al.*, 2002), but differences were found in resensitization and recycling between two receptors. The internalized NK_3, with its low-affinity interaction with β-arrestins, recycles and resensitizes rapidly (30 min), whereas the internalized NK_1, which interacts with β-arrestins with high-affinity, slowly (hours) recycles and resensitizes (Schmidlin *et al.*, 2002; 2003). Therefore, RO4583298 could bring the advantage of suppressing fully both NK_1 and NK_3 signalling in neurones expressing both receptors.

In vitro electrophysiological recordings have previously demonstrated that the selective NK_3 agonist senktide increases the firing rate of the DA neurones of SNpc and that osanetant and talnetant are able to inhibit the senktide-induced potentiation of spontaneous activity of

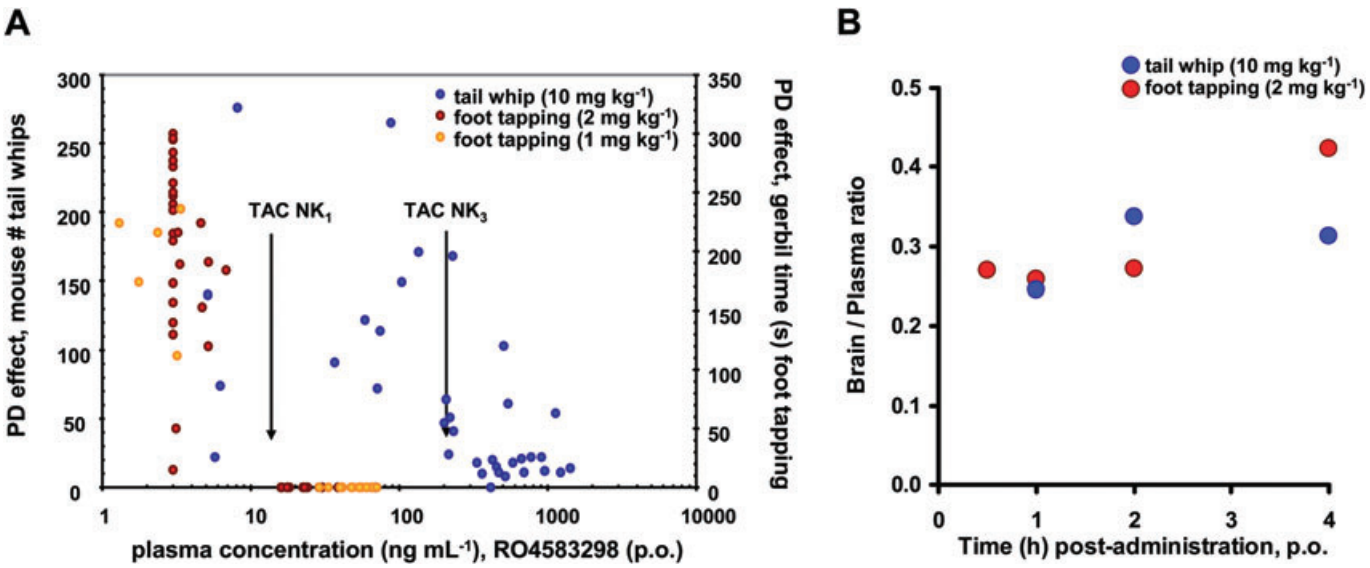

Figure 10

Pharmacokinetic/pharmacodynamic studies of the inhibitory effect of RO4583298 on NK_1 agonist GR73632-induced gerbil foot tapping and NK_3 agonist senktide-induced mouse tail whip behaviours. A. RO4583298 was administered to gerbils (1 mg·kg^{-1} or 2 mg·kg^{-1} p.o. + 3 pmol 5 μL^{-1} of GR73632 i.c.v.; n = 4–8 gerbils per group) and in mice (10 mg·kg^{-1} p.o. + 0.05 nmol 5 μL^{-1} of senktide i.c.v.; n = 5–8 mice per group), and the *in vivo* activity of RO4583298 and respective plasma concentration at various times post-administration were measured as described in the Methods. Arrows indicate therapeutic active concentration (TAC) of RO4583298 in gerbil foot tapping and mouse tail whip assays. B. Brain/plasma ratios of RO4583298 during GFT and MTW time course studies.

dopaminergic neurones (Nalivaiko *et al.*, 1997; Dawson *et al.*, 2008). In the current study, the effect of RO4583298 on firing frequency of gp SNpc DA neurones was examined by extracellular recordings. In the SNpc, the majority of neurones fired action potentials with a slow frequency and were sensitive to quinpirole, a D_2 receptor agonist. Senktide increased the basal firing frequency of responsive SNpc DA neurones in concentration-response experiments, with a pEC_{50} of 8.70. RO4583298 completely antagonized the effect of senktide on firing frequency of DA neurones in the SNpc. However, the mechanism of action of RO4583298 was apparently non-competitive since, in contrast to talnetant, high concentrations of senktide were not effective in the presence of the drug. This apparent non-competitive behaviour of RO4583298 is in good agreement with its pseudo-irreversible mode of antagonism for gpNK_3, which was seen in Schild plot analyses using the [^{3}H]-IP assay. RO4583298 had no intrinsic effect on the spontaneous activity of SNpc DA neurones suggesting that NK_3 receptors are not constitutively active in DA neurones from brain slices.

Since NK receptor pharmacology and sequence similarity of gerbils are the closest to human NK receptor pharmacology (Leffler *et al.*, 2009), we used gerbils to assess the *in vivo* activity of RO4583298. As shown previously, the i.c.v. administration of the highly selective NK_1 agonist, GR73632, in gerbil produced a characteristic rhythmic tapping of the hind feet and this behaviour was robustly inhibited by aprepitant (Hale *et al.*, 1998; Ballard *et al.*, 2001). The GFT behaviour is highly specific to NK_1, since another highly selective NK_1 antagonist, CP-99 994 was able to block it, but not its less active enantiomer (CP-100 263) (Rupniak and Williams, 1994). Therefore, the GFT assay was used to assess the *in vivo* efficacy of RO4583298 at NK_1. RO4583298 robustly blocked the GFT response in a dose-dependent manner with an ED_{50} value of 0.4 mg·kg^{-1} (p.o.) and with a long-lasting *in vivo* effect ($t_{1/2}$ = 14 h). Interestingly, this long-lasting functional GFT inhibition by RO4583298 coincides well with its pseudo-irreversible mode of antagonism observed *in vitro*.

The locomotor activity induced by i.c.v. administration of senktide in gerbils has been characterized and shown to be an appropriate model to test *in vivo* efficacy of NK_3 antagonists (Nordquist *et al.*, 2008b). Yet, the hyperlocomotion induced by senktide was also potentiated by an NK_1 antagonist aprepitant (an effect which is significant at a lower concentration of senktide, 0.03 nmol·L^{-1}); therefore, senktide-induced locomotor activity in the gerbil was not a suitable model for assessing *in vivo* efficacy of RO4583298 at the NK_3 receptor. Previous studies have established that the tail whip behaviour induced by senktide in mouse can be used as a reliable assay to quantify the *in vivo* activity of NK_3 antagonists (Nordquist *et al.*, 2010). The senktide-induced tail whip response has been shown to be fully dependent upon NK_3-mediated activation: (i) senktide was not able to induce tail whips in NK_3 knockout mice (Nordquist *et al.*, 2010); and (ii) the senktide-induced tail whip response was attenuated by selective NK_3 antagonists, SB222200, talnetant and osanetant, but not by the NK_1 antagonist aprepitant (Sarau *et al.*, 1997; 2000; Nordquist *et al.*, 2010). In the current study, RO4583298 inhibited in a dose-dependent manner the senktide-induced tail whip behaviour with an ED_{50} value of 9.0 mg·kg^{-1} and *in vivo* $t_{1/2}$ of 5 h. Pharmacokinetical/pharmacodynamical studies indicated a good agreement between the plasma concentration of RO4583298 and its inhibitory effect (ED_{50} values) in both NK_1- and NK_3- mediated effects in animal models. A plasma

concentration of 15 ng·mL^{-1} of RO4583298 is required for complete inhibition of GR73632-induced foot tapping in gerbil compared to a 200 ng·mL^{-1} plasma concentration for completely blocking senktide-induced tail whip behaviour in mouse. In view of its *in vivo* activity at mouse NK_3 and also its high-affinity bindings to NK_3 receptors of mouse and rat, which are a more acceptable species for behavioural testing, in the future RO4583298's antipsychotic properties will be determined in mouse and rat models of psychosis. Furthermore, the effect of its NK_1 antagonism, which could bring additional benefit for schizophrenia i.e. improved mood, will be characterized.

In conclusion, we observed a good correlation between *in vivo* activity of RO4583298 in gerbil and mouse and its mode of antagonism. The pseudo-irreversible mode of antagonism at gNK_1 probably contributed to RO4583298's robust and prolonged *in vivo* activity in the gNK_1 agonist-induced foot tapping model, while RO4583298's apparent partial non-competitive mode of antagonism, with its shorter *in vivo* efficacy at mNK_3, was demonstrated by a ~20-fold higher dose required in order to produce *in vivo* activity in the mouse senktide-induced tail whip model. Therefore, RO4583298 is a high-affinity, dual antagonist with an apparent non-competitive mode of antagonism and *in vivo* activity at both NK_1 and NK_3 receptors. Thus, RO4583298 could prove useful when investigating the roles of NK_1 and NK_3 receptors in psychiatric disorders such as anxiety, depression and schizophrenia.

Acknowledgements

We are grateful to Brigitte Algeyer, Philipp Ernst, Marie Haman, Catherine Hamm, Urs Humbel, Claudia Kratzeisen, Anne Marcuz, Alain Rudler, Stefanie Saenger, Michael Weber and Roger Wyler for their excellent technical assistance.

Conflicts of interest

All authors are employees of F. Hoffmann-La Roche Ltd.

References

Acsady L, Katona I, Gulyas AI, Shigemoto R, Freund TF (1997). Immunostaining for substance P receptor labels GABAergic cells with distinct termination patterns in the hippocampus. J Comp Neurol 378: 320–336.

Alexander SP, Mathie A, Peters JA (2008). Guide to Receptors and Channels (GRAC), 3rd edition. Br J Pharmacol 153: S1–S209.

Almeida TA, Rojo J, Nieto PM, Pinto FM, Hernandez M, Martin JD *et al.* (2004). Tachykinins and tachykinin receptors: structure and activity relationships. Curr Med Chem 11: 2045–2081.

Ballard TM, Sanger S, Higgins GA (2001). Inhibition of shock-induced foot tapping behaviour in the gerbil by a tachykinin NK1 receptor antagonist. Eur J Pharmacol 412: 255–264.

Blier P, Gobbi G, Haddjeri N, Santarelli L, Mathew G, Hen R (2004). Impact of substance P receptor antagonism on the serotonin and norepinephrine systems: relevance to the antidepressant/anxiolytic response. J Psychiatry Neurosci 29: 208–218.

Cao YQ, Mantyh PW, Carlson EJ. Gillespie AM, Epstein CJ, Basbaum AL (1998). Primary afferent tachykinins are required to experience moderate to intense pain. Nature 392: 390–394.

Chung FZ, Wu LH, Tian Y, Vartanian MA, Lee H, Bikker J *et al.* (1995). Two classes of structurally different antagonists display similar species preference for the human tachykinin neurokinin3 receptor. Mol Pharmacol 48: 711–716.

Dawson LA, Cato KJ, Scott C, Watson JM, Wood MD, Foxton R *et al.* (2008). In vitro and in vivo characterization of the non-peptide NK3 receptor antagonist SB-223412 (talnetant): potential therapeutic utility in the treatment of schizophrenia. Neuropsychopharmacology 33: 1642–1652.

Ebner K, Muigg P, Singewald G, Singewald N (2008). Substance P in stress and anxiety: NK-1 receptor antagonism interacts with key brain areas of the stress circuitry. Ann N Y Acad Sci 1144: 61–73.

Ebner K, Sartori SB, Singewald N (2009). Tachykinin receptors as therapeutic targets in stress-related disorders. Curr Pharm Des 15: 1647–1674.

Emonds-Alt X, Bichon D, Ducoux JP, Heaulme M, Miloux B, Poncelet M *et al.* (1995). SR 142801, the first potent non-peptide antagonist of the tachykinin NK3 receptor. Life Sci 56: PL27–PL32.

Evangelista S (2005). Talnetant GlaxoSmithKline. Curr Opin Investig Drugs 6: 717–721.

Grace AA, Onn SP (1989). Morphology and electrophysiological properties of immunocytochemically identified rat dopamine neurons recorded in vitro. J Neurosci 9: 3463–3481.

Grady EF, Garland AM, Gamp PD, Lovett M, Payan DG, Bunnett NW (1995). Delineation of the endocytic pathway of substance P and its seven-transmembrane domain NK1 receptor. Mol Biol Cell 6: 509–524.

Hale JJ, Mills SG, MacCoss M, Finke PE, Cascieri MA, Sadowski S *et al.* (1998). Structural optimization affording 2-(R)-(1-(R)-3, 5-bis(trifluoromethyl)phenylethoxy)-3-(S)-(4-fluoro)phenyl-4-(3-oxo-1,2,4-triazol-5-yl)methylmorpholine, a potent, orally active, long-acting morpholine acetal human NK-1 receptor antagonist. J Med Chem 41: 4607–4614.

Harrison PJ (1999). The neuropathology of schizophrenia. A critical review of the data and their interpretation. Brain 122: 593–624.

Hill R (2000). NK1 (substance P) receptor antagonists – why are they not analgesic in humans? Trends Pharmacol Sci 21: 244–246.

Hoffmann T, Koblet A, Peters J-U, Schnider P, Sleight A, Stadler H (2005). Preparation of 2-phenyl-N-(pyridin-3-yl)-N-methylisobutyramide derivatives as dual NK1/NK3 antagonists for treating schizophrenia. WO 2005/002577 A1.

Jenkinson KM, Mann PT, Southwell BR, Furness JB (2000). Independent endocytosis of the NK(1) and NK(3) tachykinin receptors in neurons of the rat myenteric plexus. Neuroscience 100: 191–199.

Koutcherov Y, Ashwell KW, Paxinos G (2000). The distribution of the neurokinin B receptor in the human and rat hypothalamus. Neuroreport 11: 3127–3131.

Langlois X, Wintmolders C, te Riele P, Leysen JE, Jurzak M (2001). Detailed distribution of Neurokinin 3 receptors in the rat, guinea pig and gerbil brain: a comparative autoradiographic study. Neuropharmacology 40: 242–253.

Lecci A, Maggi CA (2003). Peripheral tachykinin receptors as potential therapeutic targets in visceral diseases. Expert Opin Ther Targets 7: 343–362.

Leffler A, Ahlstedt I, Engberg S, Svensson A, Billger M, Oberg L *et al.* (2009). Characterization of species-related differences in the pharmacology of tachykinin NK receptors 1, 2 and 3. Biochem Pharmacol 77: 1522–1530.

Leucht S, Wahlbeck K, Hamann J, Kissling W (2003). New generation antipsychotics versus low-potency conventional antipsychotics: a systematic review and meta-analysis. Lancet 361: 1581–1589.

Liem-Moolenaar M, Gray FA, de Visser SJ, Franson KL, Schoemaker RC, Schmitt JA *et al.* (2010). Psychomotor and cognitive effects of a single oral dose of talnetant (SB223412) in healthy volunteers compared with placebo or haloperidol. J Psychopharmacol 24: 73–82.

Lindstrom E, von Mentzer B, Pahlman I, Ahlstedt I, Uvebrant A, Kristensson E *et al.* (2007). Neurokinin 1 receptor antagonists: correlation between in vitro receptor interaction and in vivo efficacy. J Pharmacol Exp Ther 322: 1286–1293.

Lowe JA 3rd, Drozda SE, Snider RM, Longo KP, Zorn SH, Morrone J *et al.* (1992). The discovery of (2S,3S)-cis-2-(diphenylmethyl)-N-[(2-methoxyphenyl)methyl]-1- azabicyclo[2.2.2]-octan-3-amine as a novel, nonpeptide substance P antagonisst. J Med Chem 35: 2591–2600.

Malherbe P, Bissantz C, Marcuz A, Kratzeisen C, Zenner MT, Wettstein JG *et al.* (2008). Me-talnetant and osanetant interact within overlapping but not identical binding pockets in the human tachykinin neurokinin 3 receptor transmembrane domains. Mol Pharmacol 73: 1736–1750.

Malherbe P, Kratzeisen C, Marcuz A, Zenner MT, Nettekoven MH, Ratni H *et al.* (2009). Identification of a Critical Residue in the Transmembrane Domain 2 of Tachykinin Neurokinin 3 Receptor Affecting the Dissociation Kinetics and Antagonism Mode of Osanetant (SR 142801) and Piperidine-Based Structures. J Med Chem 52: 7103–7112.

Marco N, Thirion A, Mons G, Bougault I, Le Fur G, Soubrie P *et al.* (1998). Activation of dopaminergic and cholinergic neurotransmission by tachykinin NK3 receptor stimulation: an in vivo microdialysis approach in guinea pig. Neuropeptides 32: 481–488.

Maubach KA, Martin K, Smith DW, Hewson L, Frankshun RA, Harrison T *et al.* (2001). Substance P stimulates inhibitory synaptic transmission in the guinea pig basolateral amygdala in vitro. Neuropharmacology 40: 806–817.

Meltzer H, Prus A (2006). NK3 receptor antagonists for the treatment of schizophrenia. Drug Discov Today Ther Strat 3: 555–560.

Meltzer HY, Arvanitis L, Bauer D, Rein W (2004). Placebo-controlled evaluation of four novel compounds for the treatment of schizophrenia and schizoaffective disorder. Am J Psychiatry 161: 975–984.

Mileusnic D, Lee JM, Magnuson DJ, Hejna MJ, Krause JE, Lorens JB *et al.* (1999a). Neurokinin-3 receptor distribution in rat and human brain: an immunohistochemical study. Neuroscience 89: 1269–1290.

Mileusnic D, Magnuson DJ, Hejna MJ, Lorens JB, Lorens SA, Lee JM (1999b). Age and species-dependent differences in the neurokinin B system in rat and human brain. Neurobiol Aging 20: 19–35.

Nagano M, Saitow F, Haneda E, Konishi S, Hayashi M, Suzuki H (2006). Distribution and pharmacological characterization of primate NK-1 and NK-3 tachykinin receptors in the central nervous system of the rhesus monkey. Br J Pharmacol 147: 316–323.

Nalivaiko E, Michaud JC, Soubrie P, Le Fur G, Feltz P (1997). Tachykinin neurokinin-1 and neurokinin-3 receptor-mediated responses in guinea-pig substantia nigra: an in vitro electrophysiological study. Neuroscience 78: 745–757.

Nordquist RE, Delenclos M, Ballard TM, Savignac H, Pauly-Evers M, Ozmen L *et al.* (2008a). Cognitive performance in neurokinin 3 receptor knockout mice. Psychopharmacology (Berl) 198: 211–220.

Nordquist RE, Durkin S, Jacquet A, Spooren W (2008b). The tachykinin NK3 receptor agonist senktide induces locomotor activity in male Mongolian gerbils. Eur J Pharmacol 600: 87–92.

Nordquist RE, Ballard TM, Algeyer B, Pauly-Evers M, Ozmen L, Spooren W (2010). Pharmacological characterization of senktide-induced tail whips. Neuropharmacology 58: 259–267.

Ogier R, Raggenbass M (2003). Action of tachykinins in the rat hippocampus: modulation of inhibitory synaptic transmission. Eur J Neurosci 17: 2639–2647.

Otsuka M, Yoshioka K (1993). Neurotransmitter functions of mammalian tachykinins. Physiol Rev 73: 229–308.

Peters JU, Hoffmann T, Schnider P, Stadler H, Koblet A, Alker A *et al.* (2010). Discovery of potent, balanced and orally active dual NK1/NK3 receptor ligands. Bioorg Med Chem Lett 20: 3405–3408.

Quartara L, Altamura M, Evangelista S, Maggi CA (2009). Tachykinin receptor antagonists in clinical trials. Expert Opin Investig Drugs 18: 1843–1864.

Ribeiro-da-Silva A, Hokfelt T (2000). Neuroanatomical localisation of Substance P in the CNS and sensory neurons. Neuropeptides 34: 256–271.

Rigby M, O'Donnell R, Rupniak NM (2005). Species differences in tachykinin receptor distribution: further evidence that the substance P (NK1) receptor predominates in human brain. J Comp Neurol 490: 335–353.

Rupniak NMJ, Williams AR (1994). Differential inhibition of foot tapping and chromodacryorrhoea in gerbils by CNS penetrant and non-penetrant tachykinin NK1 receptor antagonists. Eur J Pharmacol 265: 179–183.

Santarelli L, Gobbi G, Debs PC, Sibille ET, Blier P, Hen R *et al.* (2001). Genetic and pharmacological disruption of neurokinin 1 receptor function decreases anxiety-related behaviors and increases serotonergic function. Proc Natl Acad Sci USA 98: 1912–1917.

Sarau HM, Griswold DE, Potts W, Foley JJ, Schmidt DB, Webb EF *et al.* (1997). Nonpeptide tachykinin receptor antagonists: I. Pharmacological and pharmacokinetic characterization of SB 223412, a novel, potent and selective neurokinin-3 receptor antagonist. J Pharmacol Exp Ther 281: 1303–1311.

Sarau HM, Griswold DE, Bush B, Potts W, Sandhu P, Lundberg D *et al.* (2000). Nonpeptide tachykinin receptor antagonists. II. Pharmacological and pharmacokinetic profile of SB-222200, a central nervous system penetrant, potent and selective NK-3 receptor antagonist. J Pharmacol Exp Ther 295: 373–381.

Sarau HM, Feild JA, Ames RS, Foley JJ, Nuthulaganti P, Schmidt DB *et al.* (2001). Molecular and pharmacological characterization of the murine tachykinin NK(3) receptor. Eur J Pharmacol 413: 143–150.

Schmidlin F, Dery O, Bunnett NW, Grady EF (2002). Heterologous regulation of trafficking and signaling of G protein-coupled receptors: beta-arrestin-dependent interactions between neurokinin receptors. Proc Natl Acad Sci USA 99: 3324–3329.

Schmidlin F, Roosterman D, Bunnett NW (2003). The third intracellular loop and carboxyl tail of neurokinin 1 and 3 receptors determine interactions with beta-arrestins. Am J Physiol Cell Physiol 285: C945–C958.

Shughrue PJ, Lane MV, Merchenthaler I (1996). In situ hybridization analysis of the distribution of neurokinin-3 mRNA in the rat central nervous system. J Comp Neurol 372: 395–414.

Spooren W, Riemer C, Meltzer H (2005). Opinion: NK3 receptor antagonists: the next generation of antipsychotics? Nat Rev Drug Discov 4: 967–975.

Stoessl AJ (1994). Localization of striatal and nigral tachykinin receptors in the rat. Brain Res 646: 13–18.

Tamminga CA, Holcomb HH (2005). Phenotype of schizophrenia: a review and formulation. Mol Psychiatry 10: 27–39.

Tooney PA, Au GG, Chahl LA (2000). Localisation of tachykinin NK1 and NK3 receptors in the human prefrontal and visual cortex. Neurosci Lett 283: 185–188.

Urban LA, Fox AJ (2000). NK1 receptor antagonists – are they really without effect in the pain clinic? Trends Pharmacol Sci 21: 462–464.

Wu LH, Vartanian MA, Oxender DL, Chung FZ (1994). Identification of methionine134 and alanine146 in the second transmembrane segment of the human tachykinin NK3 receptor as reduces involved in species-selective binding to SR 48968. Biochem Biophys Res Commun 198: 961–966.